

IDENTIFICATION OF INVASIVE AND METASTATIC POTENTIAL OF TPL-2
KNOCKOUT KERATINOCYTES

By

Sarah Jung

Submitted to the

Faculty of the College of Arts and Sciences

of American University

in Partial Fulfillment of

the Requirements for the Degree of

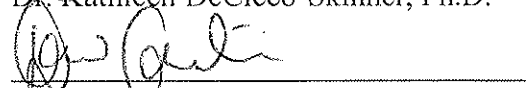
Masters of Science

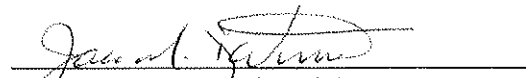
In


Biology

Chair:

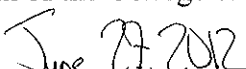

Dr. Kathleen DeCicco-Skinner, Ph.D.


Dr. David Carlini, Ph.D.


Dr. Jason D'Antonio, Ph.D.



Dean of the College of Arts and Sciences



Date

2012

American University

Washington, D.C. 20016

© COPYRIGHT

by

Sarah Jung

2012

ALL RIGHTS RESERVED

DEDICATION

I dedicate this thesis to my mother and father, Janice Anderson and Richard Jung, for their
everlasting support and inspiration.

IDENTIFICATION OF INVASIVE AND METASTATIC POTENTIAL OF TPL-2 KNOCKOUT KERATINOCYTES

BY

Sarah Jung

ABSTRACT

Tpl-2/MAP3K8 is a serine/threonine protein kinase that can activate the transcription of target genes involved in pathways associated with mitosis, cellular differentiation, apoptosis, and inflammation. Our laboratory has previously identified that mice missing the Tpl-2 gene (Tpl-2 knockout mice) are more susceptible to the development of skin cancer—the most prevalent cancer in the United States. However, it is unknown whether the squamous skin cancers that develop in Tpl-2 knockout mice have more potential to become invasive than those skin tumors that form in normal mice. Therefore, in this thesis, we compared the invasive and metastatic potential of skin cells (keratinocytes) from normal and Tpl-2 knockout mice with stimulation and genetic alterations like constitutively-activated Ras. Using various techniques including microarray, real-time polymerase chain reaction, and zymography we found MMP-9, a well-known protease associated with metastatic cells, to be up-regulated at the RNA level. Also, while Tpl-2^{+/+} keratinocytes migrate faster than Tpl-2^{-/-} in an *in vitro* scratch assay with H-Ras-infection and Mitomycin C, Tpl-2^{-/-} keratinocytes have a higher malignant conversion rate and better potential for angiogenic ability when the Ras oncogene is constitutively activated. These experiments provide evidence that Tpl-2^{-/-} keratinocytes, in conjunction with mutant Ras, show potential to become aggressive and invasive.

ACKNOWLEDGEMENTS

There are numerous people who have both helped me with these experiments and guided me through this process. First and foremost, I want to thank Dr. DeCicco-Skinner for her creativity, perseverance, thoughtfulness, and patience with me throughout my whole experience as a Masters student. At American University, I would like to thank Dr. Carlini for his Bioinformatics class and help with the microarray experiment, Curtis Gwilliam, Tracy Tabib, and Hepzi Alexander for their wonderful assistance with experiments and support in completing everything at hand on time, and Taylor Dempsey for her help with the real-time polymerase chain reaction runs. At NIH, I would like to thank Caroline Garber for her assistance in the lab, Louwei Li and Padmakumar Velayuthan Chellammal for their assistance with the IncuCyte program and scratch assay, Stuart Yuspa for his assistance and advice with the conversion assay, Cristophe Cataisson for his assistance in nearly everything including with the microscope, the tubulogenesis assay, and tissue culture advice, and Jonathan Wiest for his constant support and for pushing me through the microarray project. Biological research is a collaborative effort, and I could not have succeeded without any of them. Thank you again.

TABLE OF CONTENTS

ABSTRACT.....	ii
ACKNOWLEDGEMENTS.....	iii
LIST OF TABLES.....	vi
LIST OF ILLUSTRATIONS.....	vii
CHAPTER 1 BACKGROUND.....	1
CHAPTER 2 OBJECTIVES AND SIGNIFICANCE.....	24
Objective 1.....	24
Objective 2.....	24
CHAPTER 3 MATERIALS AND METHODS.....	25
Chemicals, Reagents, and Instruments.....	25
Animals.....	26
Newborn Mice Skin Removal.....	26
Keratinocyte Preparation, Isolation, and Plating.....	27
TPA Treatment, H-Ras-transduction, Mitomycin C and MNNG Treatment, and MAP3K8 Overexpression.....	28
RNA Extraction and Isolation.....	30
Affymetrix Microarray Preparation and Preliminary Data Filtering.....	31
Zymography Preparation and Protocol.....	32
Real-time Polymerase Chain Reaction (qPCR) Preparation and Protocol.....	34
<i>In vitro</i> Scratch/wound Healing Assay Preparation and Protocol.....	35
<i>In vitro</i> Conversion Assay Preparation and Protocol.....	36
<i>In vitro</i> Angiogenesis/tubulogenesis Assay Preparation and Protocol.....	37
Microarray Data Analysis.....	38
qPCR Data Analysis.....	39

Scratch Assay Data Analysis using IncuCyte	39
<i>In vitro</i> Conversion Assay Data Analysis	39
CHAPTER 4 RESULTS	40
Microarray.....	40
Global Results and Initial Filtering for Significant Gene Comparison between Genotypes Associated with TPA Treatment.....	40
MMP-2, MMP-3, MMP-9, Lipocalin-2, and TIMPs: MMP-9 is Up-regulated in Tpl-2 ^{-/-} Samples, while TIMP-2 is Down-regulated with TPA Treatment	44
Real-time Polymerase Chain Reaction for MMP-2 and MMP-9.....	47
Zymography	48
<i>In vitro</i> Wound Healing/scratch Assay	50
<i>In vitro</i> Malignant Conversion Assay	53
<i>In vitro</i> Tubulogenesis Assay.....	55
CHAPTER 5 DISCUSSION.....	59
Genes Associated with Cellular Invasiveness like MMP-2 and MMP-9 are Up-regulated at the RNA Level in Tpl-2 ^{-/-} Mouse Keratinocytes	59
Tpl-2 ^{-/-} Keratinocytes May Migrate Slower when Cell Replication is Inhibited, but their Higher Conversion Rate and Higher Tube Formation with Mutated Ras Suggest Potential for Aggressiveness and Metastasis in Mouse Skin	62
Future Experiments and Directions	66
CHAPTER 6 CONCLUSIONS	70
REFERENCES	71

LIST OF TABLES

Table

Table 1: Type of Skin Growths.....	3
Table 2: Clinical Stages of BCC and SCC and Melanoma, from the National Cancer Institute, 2010	6
Table 3: qPCR Primers for MMP-2, MMP-9, and β -actin	34
Table 4: Significant Genes based on Genotypic Differences	46
Table 5: Gelatin Zymography Densitometry Results	49
Table 6: Conversion Assay Results	53
Table 7: Quantitative Tubulogenesis Assay Results.....	57
Table 8: Conversion Gelatin Zymography Densitometry Results	68

LIST OF ILLUSTRATIONS

Figure

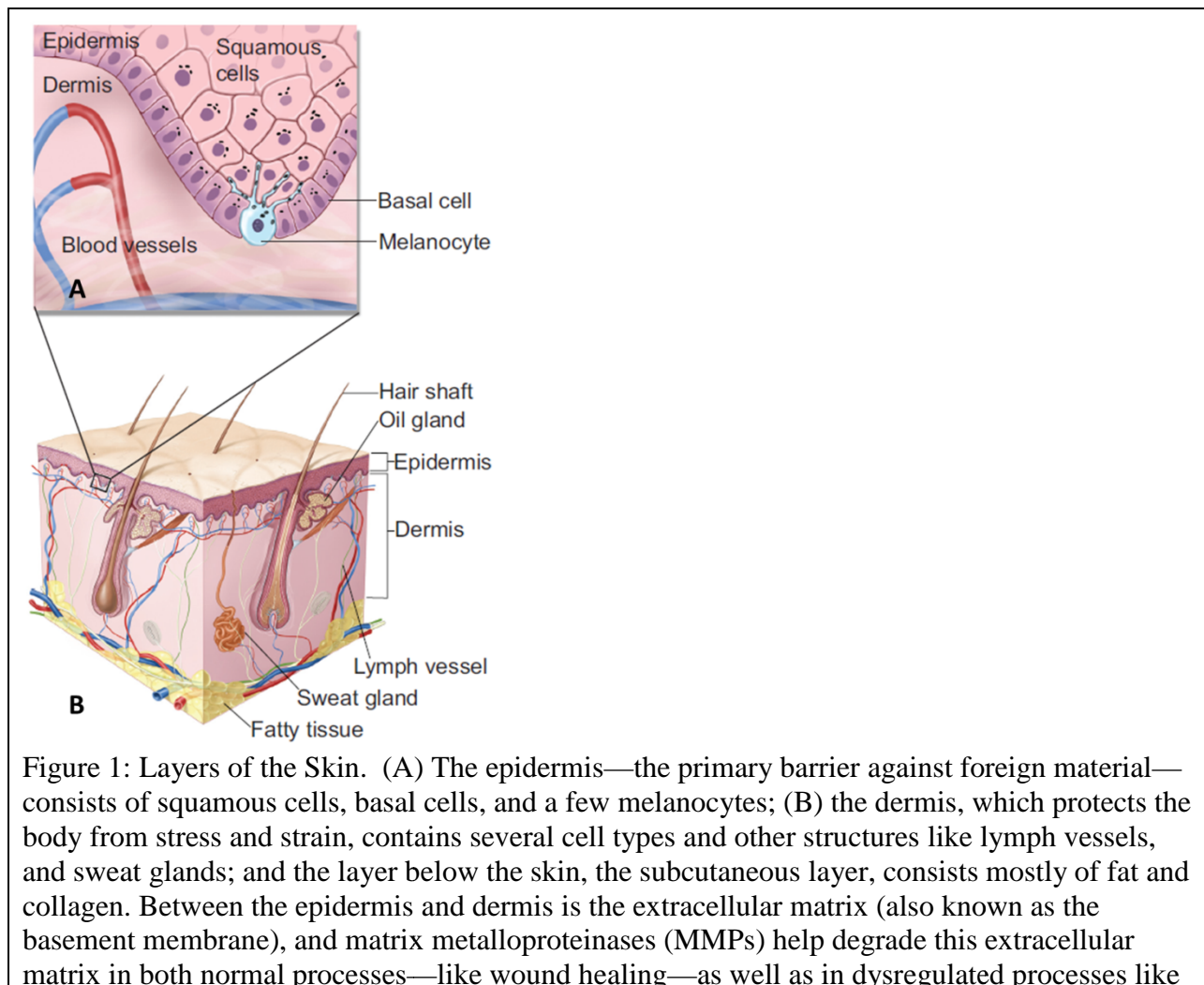
Figure 1: Layers of the Skin.....	1
Figure 2: The Seven Hallmarks of Cancer.....	3
Figure 3: Skin Growths Associated with BCC and SCC.....	5
Figure 4: Images of Melanoma.....	5
Figure 5: Canonical and Non-canonical NF- κ B Activation Pathways.....	8
Figure 6: The NF- κ B1, ABIN-2, and MAP3K8/Tpl-2 ternary complex.....	10
Figure 7: The Activation of NF- κ B1 and Subsequent Cell Cycle Progression and Apoptosis Inhibition.....	10
Figure 8: Matrix Metalloproteinase Activation.....	14
Figure 9: The Wound Healing Process.....	15
Figure 10: MMP-9 Activation Pathway.....	17
Figure 11: The Agonist TPA and its General Activation Cascade.....	21
Figure 12: Box-whisker Plot and Profile Plot of Experimental Groups, Normalized, Log- Transformed, and Median-Centered.....	41
Figure 13: MA-Plot Comparing WT 0h (Sample 1) and KO 0h (Sample 2).....	42
Figure 14: Global Heatmap of Differential Expression between Genotypes using Fold Change Filter 2 for the Three Ratios that Compared Expression between Genotypes across TPA Treatments.....	44
Figure 15: Heatmap of MMP-2, MMP-3, MMP-9, Lipocalin-2, and the TIMPs.....	45
Figure 16: Heatmaps of Significant Genes based on Genotypic Differences from the 3 Fold Change Ratios for TPA Treatment.....	45
Figure 17: Real-time Polymerase Chain Reaction Results for MMP-2 (A) and MMP-9 (B)	48
Figure 18: Gelatin Zymography with Untreated, H-Ras, TPA, and H-Ras and TPA Samples....	49
Figure 19: Scratch Assay Summary.....	51
Figure 20: Migration Differences of H-Ras-infected Keratinocytes with Cell Replication Inhibitor Mitomycin C.....	52

Figure 21: Keratinocyte Cellular Morphology and Conversion Assay Dishes after Rhodamine Staining	54
Figure 22: Tubulogenesis Assay Results	56
Figure 23: Full Blood Vessel Networks made by 3B11 Cells from Conditioned Media Samples	57
Figure 24: Heatmap with the Most Significant Genes Based on Genotypic Differences Across TPA Treatments	67
Figure 25: Gelatin Zymography with Conversion Assay Samples.....	68

CHAPTER 1

BACKGROUND

As the largest organ in the body, the skin is the first barrier against foreign pathogens and protection from heat and injury. Its other functions include water storage, insulation via fat storage, sensation, temperature regulation, and production of vitamin D (National Cancer Institute, 2010). The skin has two layers—the epidermis and dermis—and they serve two different functions. The epidermis provides water insulation and is the primary barrier against foreign material, while the connective tissue of the dermis cushions and protects the body from stress and strain (Fig. 1A-B) (National Cancer Institute, 2010).

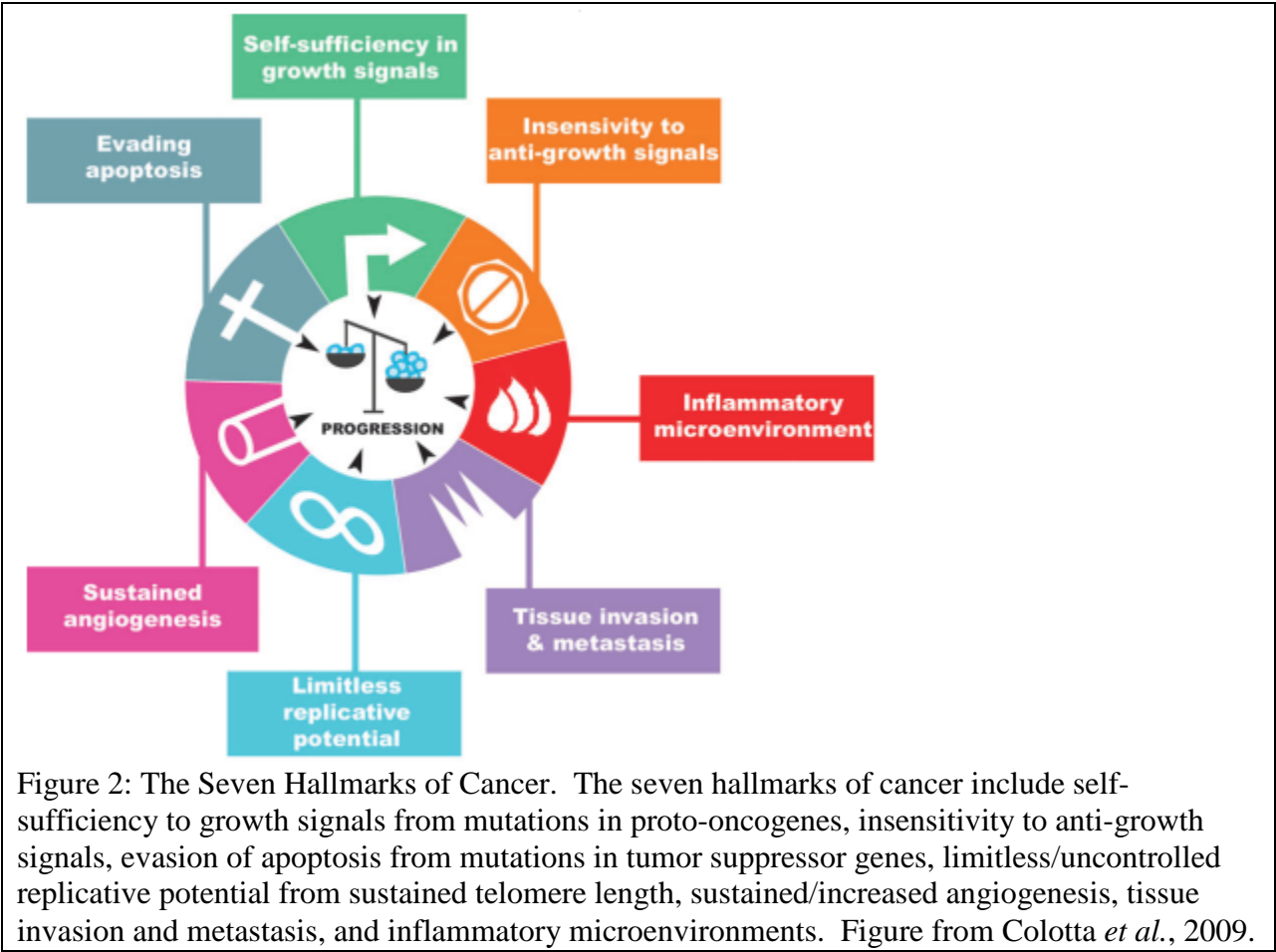


cancers that become metastatic and spread to other parts of the body. Figure from the National Cancer Institute, 2010.

The epidermis consists of the top layer of skin, mostly consisting of flat, squamous cells. Below the squamous cells are basal cells. Melanocytes are also scattered among basal cells, found deeper in the epidermis (Fig. 1A). Melanocytes produce the pigment melanin found in the skin. When the skin is exposed to ultraviolet (UV) radiation, these cells make more pigment, which is responsible for the skin darkening during sun exposure (National Cancer Institute, 2010). The skin layer below the epidermis is the dermis, and it contains several types of cells and structures such as blood vessels, lymph nodes, and glands (Fig. 1B). Sweat glands help keep the body cool and sebum glands are responsible for making sebum, a substance that keeps the skin moist, preventing it from cracking and drying out. Both sweat and sebum reach the surface of the skin through pores (National Cancer Institute, 2010). Despite their differing functions, together the epidermis and dermis provide interconnected protection for the body from internal and external factors. However, cancer can arise when new cells from the epidermis, dermis, or other areas of the body proliferate in an uncontrolled fashion or when damaged cells do not die as they should, resulting in accumulation of extra cells and subsequently forming a tumor (National Cancer Institute, 2010).

There are over 200 different types of cancer, defined as uncontrolled cell proliferation. The seven hallmarks of cancerous cells include self-sufficiency to growth signals from mutations in proto-oncogenes (genes of the cell cycle), insensitivity to antigrowth signals, evasion of programmed cell death (apoptosis) due to mutations in tumor suppressor genes, unlimited growth and proliferation potential relating to sustained chromosomal telomere length, continual angiogenesis (formation of new blood vessels), tissue evasion and metastasis, and inflammation (Hanahan and Weinberg, 2000; Colotta *et al.*, 2009). These seven main characteristics delineate

between normal and cancerous cells (Fig. 2). Skin cancer in particular has been linked to several hallmarks, including inflammation (Moore *et al.*, 1999; Colotta *et al.*, 2009).



Skin cancer is the most prevalent cancer in the United States (National Cancer Institute, 2010). However, not all skin growths are considered cancerous. Moles are common growths on skin and they rarely become tumors. However, malignant growths that do form are considered skin cancers. Skin growth differences—benign (not cancerous) and malignant (cancerous)—are presented:

Table 1: Type of Skin Growths

Type of Growth	Benign	Malignant
Examples	Moles	Basal cell carcinoma (BCC), squamous cell carcinoma (SCC), melanoma
Life threatening?	Rarely	Can be life-threatening

Removable?	Easily removable; usually does not grow back	Removable; sometimes grows back
Invasion ability	Does not invade/spread to neighboring or other tissues	May invade/spread to other tissues or areas of the body

The two most prevalent types of skin cancer are basal and squamous cell carcinomas, BCC and SCC, respectively. BCC is several times more common than SCC, but both are several times more likely to develop than melanoma. Of the primary malignancies, 77% are BCC, 20% are SCC, and 3% are melanoma (Nodwell, 2003). The last type of skin cancer, melanoma, is the deadliest form with high rates of fatality (National Cancer Institute, 2010). Another concerning aspect of melanoma is its significant increase in incidence within the past thirty years: its rate has increased over sixty percent (National Cancer Institute, 2010).

BCC begins in the basal cell layer of the skin and occurs sporadically in commonly sun-exposed areas including the face and neck. SCC begins in the top layer of the skin from squamous cells, and is also associated with sun exposure, typically seen on the face, ears, and neck. Even though SCC is slow-growing, it can become deeply invasive and can lead to metastasis from atypical squamous cells invading and migrating through the basement membrane into the dermis, potentially spreading to other parts of the body (Nodwell, 2003).

BCC and SCC are usually painless skin cancers. BCC is typically seen as small, firm lumps that can be smooth, shiny, pale, or waxy (Fig. 3A-B). Skin growths associated with SCC are flatter, red or brown spots/patches that can be rough, dry, and scaly and can bleed and crust (Fig. 3C-E).



Figure 3: Skin Growths Associated with BCC and SCC. Panels A and B are characteristic of BCC with raised, shiny, pale, or waxy growths; panels C, D, and E are characteristic of SCC in that they are flat, red or brown patches that can crust and/or bleed. Figure from the National Cancer Institute, 2010.

Melanoma begins in melanocytes (pigment cells) and is commonly found on the head, between the shoulders and hips, or on lower parts of the legs from history involving sun burns, tanning (especially with artificial UV radiation sources), and genetics. Even though all skin cancers are considered dangerous, melanoma is far more life-threatening due to its rapid ability to spread to other parts of the body and attach to form new tumors in lymph nodes, the brain, bones, and liver (National Cancer Institute, 2010). Diagnostic characteristics used for detection of melanoma involve the ABCDE acronym: asymmetrical, irrregular borders, uneven coloration, larger diameter, and evolution of a particular skin area. The texture of the growth may change in more advanced stages of melanomas as well. Melanomas are unlike BCC and SCC due to their irregular/asymmetric borders (Fig. 4A) and discolored skin growths (Fig. 4B).

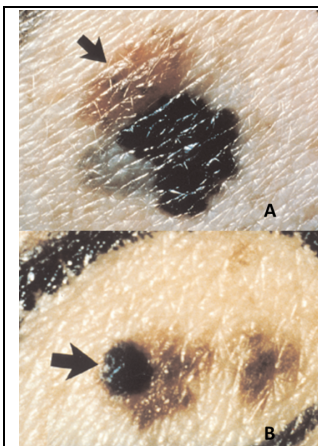


Figure 4: Images of Melanoma. This image portrays the typical characteristics seen in melanoma in the skin, including evolution of the skin growth and discoloration (A) and larger, asymmetrical diameters and irregular borders (B). Figure from the National Cancer Institute, 2010.

The diagnoses of BCC, SCC, and melanoma are most commonly through biopsies, where part or all of the potential malignant growth is removed. Physicians stage skin cancer based on size, width, and depth of the growth as well as if the cancer has spread to other parts of the body

(National Cancer Institute, 2010). The different clinical stages of cancer for BCC and SCC and melanoma are below:

Table 2: Clinical Stages of BCC and SCC and Melanoma, from the National Cancer Institute, 2010

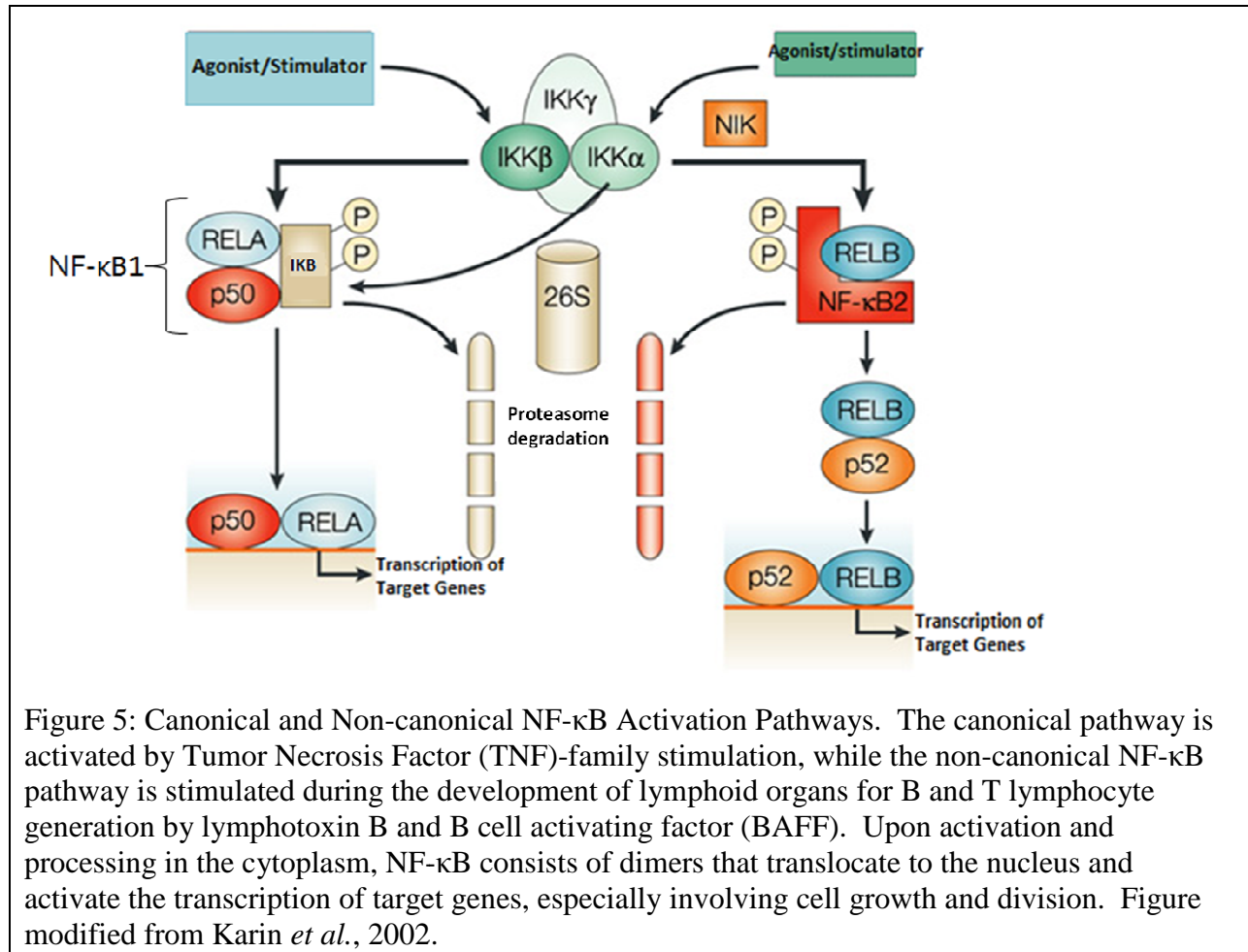
Stage of Cancer	BCC and SCC	Melanoma
Stage 0	Involves only the top layer of skin (carcinoma in situ)	Involves only the top layer of skin (melanoma in situ)
Stage I	Growth is as large as 2cm wide	Tumor is no more than 1mm wide and can be thick
Stage II	Growth is larger than 2cm wide	Tumor is between 1-2mm wide and the surface appears broken down (early sign of potential metastasis)
Stage III	Cancer has invaded below the skin to cartilage, muscle, bone, or nearby lymph nodes but has not spread to other areas	Melanoma cells have spread to at least one nearby lymph node or tissue
Stage IV	Cancer has spread to other parts of the body; BCC rarely spreads to other parts of the body, but SCC can	Melanoma cells have spread to the lungs or other organs, skin areas, or lymph nodes far away from the primary growth (also can spread to the brain, bones, or liver)

Treatments will vary based on the type of skin cancer and its clinical stage. With the intent of completely removing/destroying the cancer, the most common form of treatment is surgical removal of the growth. Surgeons remove as much of the tumor as possible while also minimizing tissue damage of normal cells. The skin growth can even be removed during the biopsy, removing some surrounding tissue as well if necessary (Stulberg *et al.*, 2004). For BCC and SCC treatments, the outcome is typically long-lasting, yielding a 95% cure rate if the tumor is primary (Nodwell, 2003). However, if the skin cancer is more advanced and has metastasized, patients may undergo further surgeries, receive radiation, and/or enter a clinical trial with novel treatment methods (National Cancer Institute, 2010). Chemotherapy may also be suggested when patients are at risk of re-emerging tumors. Chemotherapy uses drugs to kill fast-growing cancer cells at the risk of killing rapidly-dividing normal cells like blood cells, hair cells, and

cells that line the digestive tract, which can lead to unwanted side effects such as hair loss, higher susceptibility to infection, loss of appetite, and nausea (National Cancer Institute, 2010).

Tumorigenesis of malignant BCC or SCC is typically due to 4 to 6 genetic changes, often from mutations of tumor suppressors or proto-oncogenes and subsequently leading to the development of a precursor lesion. More developed malignant tumors commonly have a mutation of the Rat sarcoma (Ras) oncogene—the most frequently mutated gene in human cancers (Ratushny *et al.*, 2012). Normal Ras molecules are small GTP-binding proteins that regulate genes involving cell growth, differentiation, and survival. Thus, aberrant Ras activation via mutation leads to tumorigenesis, resistance to apoptosis, drug resistance, and angiogenesis. Ras also regulates nuclear factor kappa B (NF- κ B), which is important for cell cycle control and activation of the mitogen-activated protein kinase (MAPK) pathway (Su *et al.*, 2012).

NF- κ B is a pleiotropic transcription factor found in almost all cell types and is involved in processes like inflammation, immunity, differentiation, cell growth, tumorigenesis, and apoptosis (Karin *et al.*, 2002). Numerous stimuli can activate it and numerous genes regulate it. Thus, NF- κ B is the interface between intracellular signals and gene expression (Hayden and Ghosh, 2008). In its inactive, latent state, it is held in a cytoplasmic complex with inhibitor of kappa B (I κ B), which inhibits its activity. Upon activation via inducing stimuli, I κ B kinases (IKKs) degrade I κ B via phosphorylation, ubiquitination, and subsequent proteasomal degradation, allowing NF- κ B dimers to translocate into the nucleus where they bind to specific DNA sequences (called κ B sites) and promote the transcription of target genes like AP-1, Ets, and Stat—all of which can target gene expression relating to cell growth and division, thus stimulating the cell cycle (Gilmore, 2011). NF- κ B is involved in the canonical (classical) and non-canonical (alternative) pathways, which regulate distinct sets of genes (Fig. 5).



This thesis focuses on players involved in the classical NF-κB activation pathway and NF-κB1 activation. The canonical pathway is usually triggered in response to microbial and viral infections as well as exposure to proinflammatory cytokines (small cell-signaling molecules associated with systemic inflammation), all of which can activate the IKK complex and subsequently NF-κB1 (Karin *et al.*, 2002). Upon NF-κB1 activation via inducible phosphorylation by stimulators such as protein kinase A, IκB releases from the complex and becomes degraded, and NF-κB (also known as p105) undergoes constitutive processing through the proteasome to yield p50 (Hayden and Ghosh, 2008). Its heterodimer complex with p65 (also known as RelA)—together called NF-κB1—enter the nucleus and activate the transcription of

target genes, including immunoregulatory and inflammatory genes, anti-apoptotic genes, and genes that positively regulate cell proliferation (Karin *et al.*, 2002).

NF- κ B1 can also regulate the mitogen-activated protein kinase (MAPK) pathway through the MAP kinase kinase kinase (MAP3K) family, specifically MAP3K8 (also known as Tpl-2/Cot). NF- κ B1 represses MAP3K8-induced MAPK signaling by keeping it in a ternary complex with it and ABIN-2 (A20-binding inhibitor of NF- κ B 2) (Gilmore, 2011). Upon stimulation, MAP3K8 becomes phosphorylated and activated upon its release with NF- κ B1. NF- κ B1 then follows its usual course: proteasomal degradation and processing of p105 into the p50/p65 heterodimer, which then translocates into the nucleus and activates gene transcription. Upon activation and subsequent release from NF- κ B1 and ABIN-2, phosphorylated MAP3K8 activates and phosphorylates MAP2K8 (Mek1/2), which subsequently activates and phosphorylates MAPK8 (Erk1/2). Phosphorylated-Erk1/2 can enter the nucleus and activate the transcription of target genes such as those involved in inflammation or the cell cycle (Fig. 6). The role of ABIN-2 is currently unknown other than its role in stabilizing the complex.

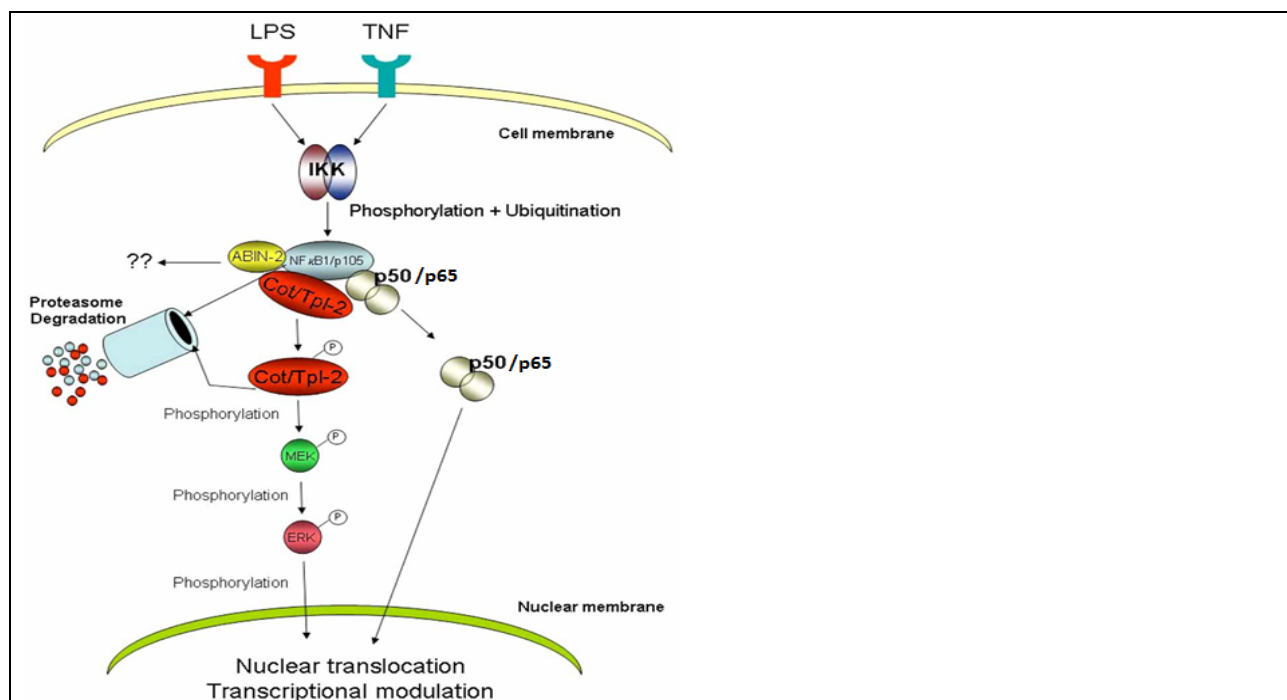


Figure 6: The NF- κ B1, ABIN-2, and MAP3K8/Tpl-2 ternary complex. Tpl-2 is not activated until its release with ABIN-2 and NF- κ B1; upon activation and complex dissociation, p50/p65 and phosphorylated-Erk translocate to the nucleus and activate the transcription of target genes relating to the cell cycle and inflammation. Figure modified from George and Salmeron, 2009.

Many of the genes that NF- κ B1 can activate are involved in signaling pathways that stimulate the proliferation of epithelial cells by the induction of cyclin D1 gene transcription, thereby activating the cell cycle (Fig. 7). AP-1 (whose transcription is regulated by NF- κ B1) binds to receptor tyrosine kinase (RTK) upon activation of the MAPK cascade and subsequently activates cyclin D1 expression, leading to cell cycle progression and apoptosis inhibition (Karin *et al.*, 2002).

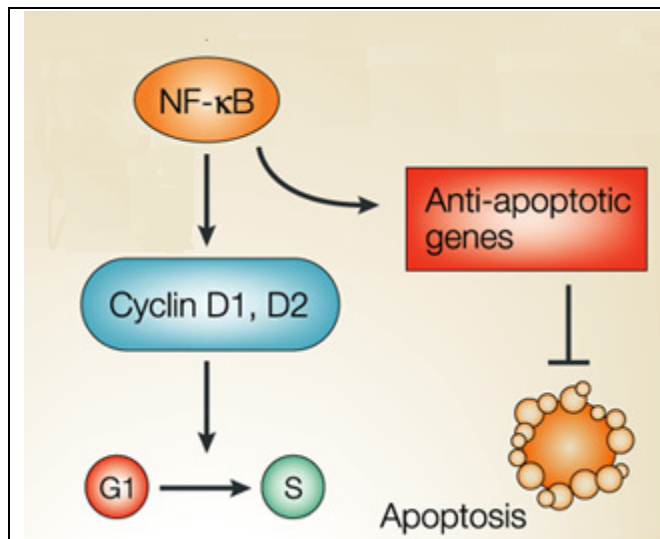


Figure 7: The Activation of NF- κ B1 and Subsequent Cell Cycle Progression and Apoptosis Inhibition. NF- κ B1 activation is involved in cell cycle progression and the inhibition of apoptosis, which have implications in cancerous environments. Figure modified from Karin *et al.*, 2002.

Through mutations from a number of genes, NF- κ B1 can become constitutively active, resulting in continual stimulation of cyclin D1 (as well as other G1 cyclins), causing enhanced and uncontrolled cell proliferation, and can lead to a number of diseases such as arthritis, chronic inflammation, asthma, neurodegenerative diseases, heart disease, and cancer (Gilmore, 2011). Especially seen in cancer, this chronic, constitutive signaling from various signals contributes to cell proliferation, abrogate growth suppression, and evasion of apoptosis.

One of the most common pathways associated with inflammation is the MAPK pathway—including MAP3K8/Tpl-2—which can regulate gene expression relating to mitosis, differentiation, apoptosis, and inflammation. In rodents, Tpl-2 is a serine/threonine kinase and as such, it prefers to phosphorylate serines and threonines, thereby activating their proteins. Transcriptional activation of target genes involved in these pathways can lead to a physiological response like inflammation from neutrophils, white blood cells associated with the immune response, which secrete proinflammatory cytokines like interleukin-1 (IL-1) and tumor necrosis factor (TNF); even though inflammation is associated with normal processes, chronic inflammation can lead to a variety of cancers and other diseases (Colotta *et al.*, 2009).

As a protein that is stimulated by inflammatory responses, MAP3K8/Tpl-2 seems to have a dual role in cancer: it is seen as a proto-oncogene in some cancer types and as a tumor suppressor in others, including skin cancer. The overexpression of Tpl-2 as an oncogene has been linked to breast cancer, lung cancer, prostate cancer, and some lymphomas (Gilmore, 2011). However, its absence leads to NF- κ B1 becoming constitutively active, which is associated with several disease-states (particularly ones involving chronic inflammation) and cancer. The loss of Tpl-2 in mice alters its associated pathways and promotes tumorigenesis due to constitutive NF- κ B1 activation.

Tpl-2^{-/-} male and female mice were initially engineered in 1997 and display no adverse phenotype compared to Tpl-2^{+/+} mice and can develop normally (Ceci *et al.*, 1997; George and Salmeron, 2009). Their bone marrow, thymus, spleen, and lymph nodes are histologically normal and have a normal ratio of all expected immune cell subsets (Dumitru *et al.*, 2000). They are also of normal size and weight, have a normal lifespan under pathogen-free conditions, and can mate and breed well for laboratory use (Gantke *et al.*, 2011). These transgenic mice are

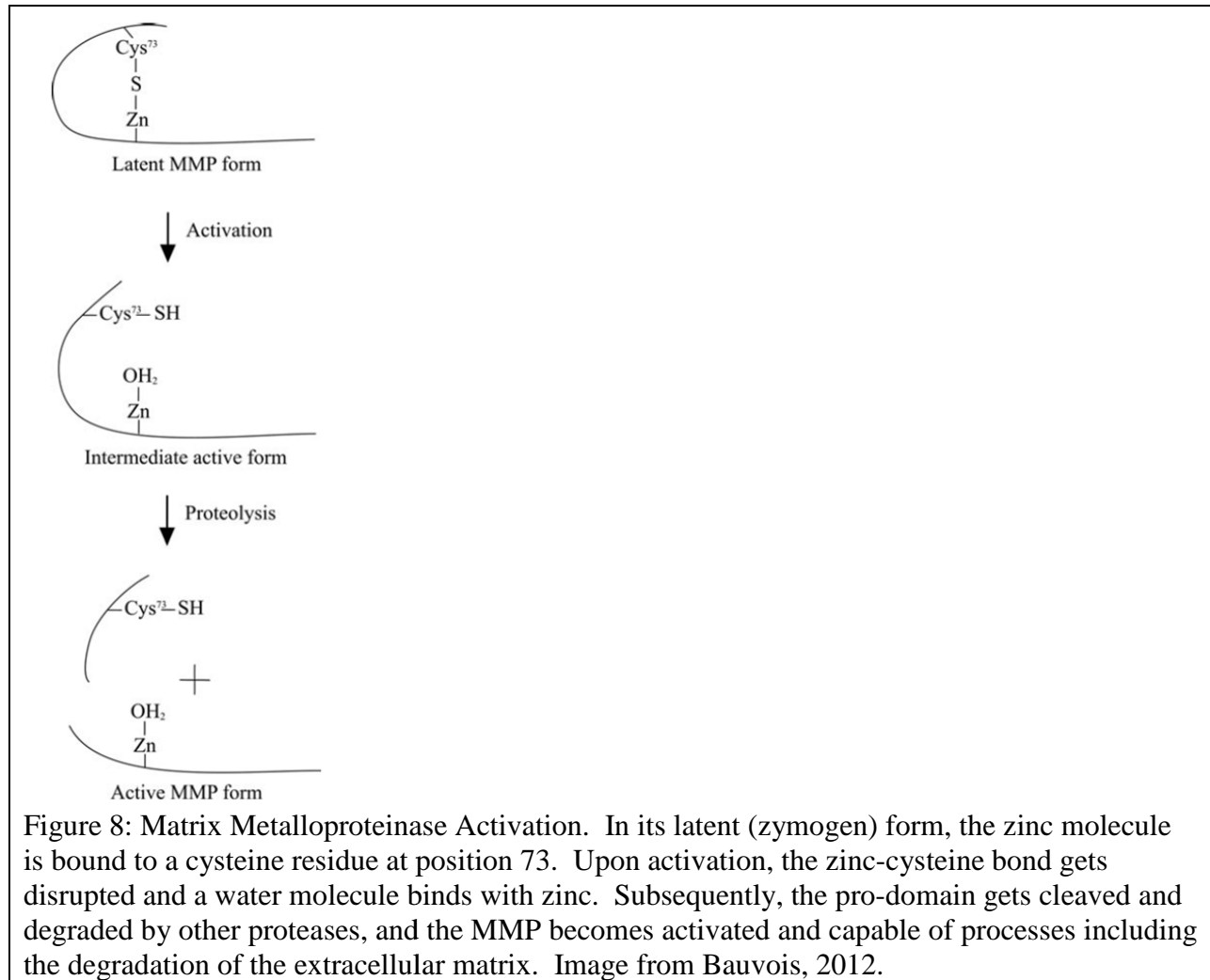
important to the field of MAPK research due to the association of Tpl-2/MAP3K8 with the canonical NF- κ B pathway. Tpl-2 could also be a potential target for the treatment of autoimmune diseases and cancer associated with chronic inflammation (George and Salmeron, 2009).

In previous and recent research, it was seen that Tpl-2^{-/-} mice have significantly more squamous skin tumor formation and higher inflammation levels than Tpl-2^{+/+} mice using the two-stage carcinogenesis model (DeCicco-Skinner *et al.*, 2010). In this experiment, mouse skin was initiated with the carcinogen 7,12-dimethylbenz-(a)anthracene (DMBA), which induces point mutations in the H-Ras oncogene. 12-O-tetradecanoylphorbol-13-acetate (TPA) treatment then promotes the initiated skin cells that have a mutant Ras oncogene, allowing these skin cells to develop into skin tumors. Skin tumors arose after approximately 12 weeks depending on the strain of the mouse (DeCicco-Skinner *et al.*, 2010). Without Tpl-2, NF- κ B1 is constitutively activated upon an inflammatory response from proinflammatory cytokines like interleukin-1 (IL-1) and tumor necrosis factor (TNF), which are secreted by neutrophils in the skin environment (DeCicco-Skinner *et al.*, 2010). These conditions can explain the heightened inflammation and increased cell cycle in Tpl-2^{-/-} skin cells in mice—epidermal cells/keratinocytes in particular. Both the increase in cell cycle and the inflammatory environment promote adequate conditions for skin tumorigenesis (Colotta *et al.*, 2009).

Even though Tpl2^{-/-} mice have a higher incidence of squamous skin tumor formation due to higher inflammatory levels, it is unknown as to whether or not these tumors have the potential to be invasive and metastatic. Previous research has shown that in Tpl-2^{-/-} mice, the transcription of key matrix metalloproteinases (MMPs) are activated via NF- κ B1 (Lin *et al.*, 2009). MMPs are zinc-dependent endopeptidases that degrade proteins by cleaving peptide bonds (Hu and

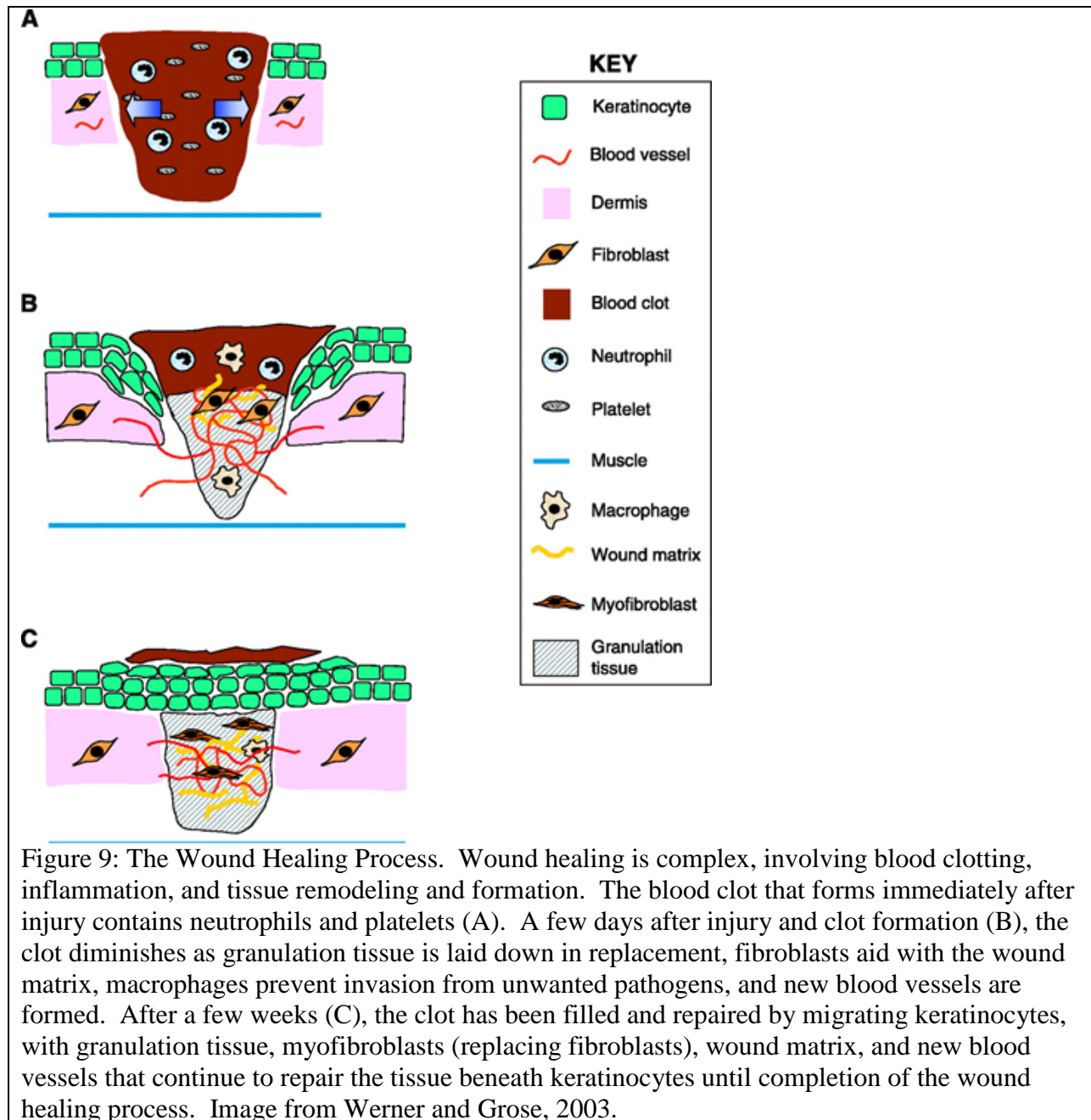
Beeton, 2010). They are particularly important in the body due to their ability to degrade all major protein components of the extracellular matrix and basement membranes. κ B sites were identified in promoters of genes (AP-1 in particular) that encode several matrix metalloproteinases, and the over-activation of NF- κ B1 contributes to extracellular matrix destruction and, hence, cancer metastasis by tumor cells (Karin *et al.*, 2002).

MMPs are known for their involvement in metastases within invasive cancers, but they are also associated with wound healing, cell movement, and a variety of other essential roles in the body. Due to their protease activity and ability to degrade the extracellular matrix and basement membranes, they are essential for normal biological processes like embryonic development, tooth development, the menstrual cycle, ovulation, and wound healing (Folgueras *et al.*, 2004). There are 23 distinct MMPs (6 different groups based on structure and substrate specificity) with varying biological roles (Snoek-van Beurden and Von den Hoff, 2005). However, they all share particular functional and structural components: a hydrophobic signal peptide for secretion, a propeptide domain for the enzyme's latency, a catalytic domain with a conserved zinc-binding site, and an intermediate hinge region (Bauvois, 2012). Tissue inhibitors of metalloproteinases (TIMPs) bind to the pro-MMP domain to prevent MMP activation; within the catalytic domain, the zinc molecule, Zn^{2+} is bound to a cysteine residue. However, when the bond between zinc and cysteine gets disrupted (called the cysteine switch), the MMP becomes activated: a water molecule binds to zinc, and the pro-MMP domain becomes cleaved autolytically, allowing the MMP to become enzymatically active (Fig. 8) (Snoek-van Beurden and Von den Hoff, 2005).



Matrix metalloproteinases are also important in skin tissue remodeling and repair (also known as wound healing). Upon the onset of a wound, neutrophils are first to invade into the wound to help with the clot, which is the cause of the swelling often seen around normal wounds (Fig. 9A). A few days after the injury, most of the neutrophils have undergone apoptosis, while macrophages—another type of white blood cell—predominate around the edge of the repaired tissue, protecting the body from infection by invading pathogens. In the meantime, endothelial cells like keratinocytes migrate into the clot, proliferating and helping with angiogenesis, and fibroblasts (cells of the dermis) proliferate and deposit new tissue of the extracellular matrix (called granular tissue). Keratinocytes proliferate at the wound edge and migrate towards each

other to re-epithelialize the damaged skin area and close the wound (Fig. 9B). A week or so post injury, the wound should be healed with granulation tissue, covered with a new epidermis while myofibroblasts, replacing fibroblasts, aid in repairing the tissue beneath with new blood vessel formation and more wound matrix to allow the wound to heal completely (Fig. 9C) (Werner and Grose, 2003).



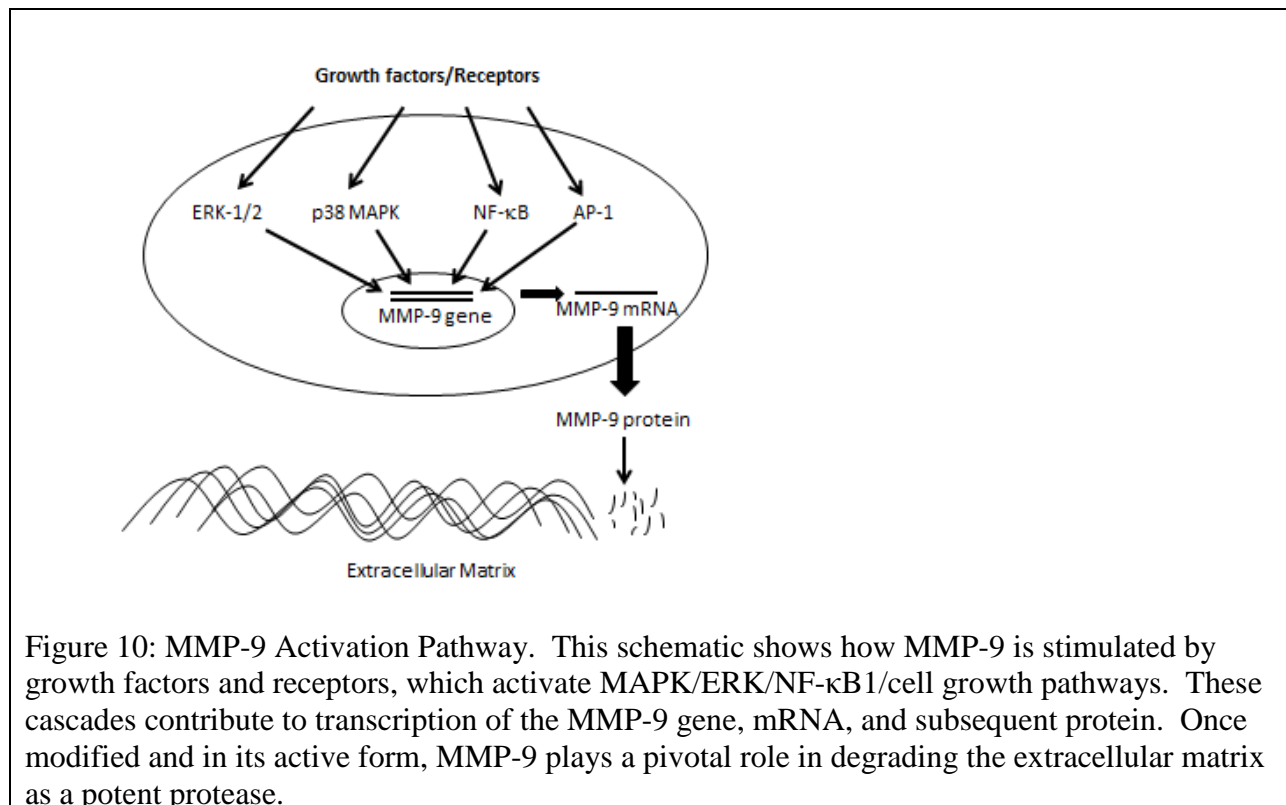
Wound healing stimulates keratinocyte and fibroblast proliferation under normal physiological conditions, helping with the synthesis and breakdown of extracellular matrix proteins as well as aiding in the regulation of the immune response. This process involves a multitude of proteins and molecules and cross-talk between pathways associated with cell proliferation, inflammation, and tissue repair (Werner and Grose, 2003). Keratinocytes are released from basal lamina, whereby they dissolve the matrix via MMP proteolysis.

Although it is typically a normal physiological response and process, wound healing can become obscured when a significant gene in a key pathway is lost, like that of Tpl-2 in mice. These genotypic differences between Tpl-2^{+/+} and Tpl-2^{-/-} cells can be observed experimentally using *in vitro* and *in vivo* wound healing experiments. Mitomycin C is an antibiotic that is also used at times in the *in vitro* wound assays because of its ability to inhibit cell replication. Therefore, the assay compares only migration/mobility differences between samples as the wound/scratch is repaired without having to consider cellular proliferation differences.

MMPs also play a pivotal role in the formation of new blood vessels both in normal and cancerous conditions (Folgueras *et al.*, 2004). In a cancerous state, MMPs promote tumor progression by enhancing angiogenesis, disrupting local tissue architecture to permit further tumor growth, and breaking down the extracellular matrix to allow metastatic tumor cells to invade and penetrate into other areas of the body (Shapiro, 1998). The gelatinases (in particular MMP-2 and MMP-9, gelatinase A and B, respectively) have shown to play crucial roles in the invasion ability of cancerous cells.

By digesting gelatin—the denatured form of collagen—the gelatinases are able to aid in the degradation of the extracellular matrix. Consequently, MMP-2 and MMP-9 have shown to be up-regulated in numerous cancer types, both at early and at advanced, malignant stages

(Snoek-van Beurden and Von den Hoff, 2005). Elevated levels of MMP-2 and MMP-9 have been seen in breast, brain, ovarian, pancreatic, colorectal, bladder, prostate, and lung cancers and melanoma as well as in several leukemias and lymphomas (Bauvois, 2012). In earlier stages of cancer, MMP-2 and MMP-9 can activate growth factors, help in evading apoptosis, and release angiogenic factors (Folgueras *et al.*, 2004). In later stages of cancer, MMP-9 in particular can influence cell behavior by activating major signaling pathways like NF- κ B1 and MAPK. However, MMP-9 can also be stimulated by these same pathways, thereby regulating pathways like cell growth, migration, invasion, inflammation, and angiogenesis and primarily causing the destruction of the extracellular matrix (Fig. 10). MMP-2 and MMP-9 are also associated with tumor aggressiveness and poor patient prognosis at later stages of cancer (Bauvois, 2012).



While the enzymatic activity of MMP-2 and MMP-9 can be inhibited by a one-to-one complex with a TIMP, MMP-9 also forms a complex with another protein that protects its enzymatic activity: neutrophil gelatinase-associated lipocalin (NGAL, or lipocalin-2—Lcn-2).

Unlike TIMPs, whose higher expression has been shown to inhibit aggressive and invasive tumor cells, the overexpression of the MMP-9/lipocalin-2 complex has also been linked independently with inflammation-associated and invasive skin cancers (Lee *et al.*, 2008). However, the enzymatic activity of MMP-9 is what is responsible for the degradation of the extracellular matrix; lipocalin-2 only protects the enzymatic activity of MMP-9 when they are in a complex with one another.

Overproduction of MMP-2 and MMP-9 is associated with tissue destruction in cancers related to chronic inflammation (Snoek-van Beurden and Von den Hoff, 2005). MMP-9 in particular is activated by neutrophils—white blood cells present in inflammatory environments—and this activation aids with the degradation of the extracellular matrix (Masson *et al.*, 2005). MMP-2 is regulated by activated protein C (APC), which also stimulates epithelial cell proliferation and plays a role in tissue repair and extracellular matrix remodeling through the MAPK signaling pathway (Xue *et al.*, 2004). In other studies, it has been shown that the MAPK pathway plays a pivotal role in melanoma and SCC development (DeCicco-Skinner *et al.*, 2010; Inamdar *et al.*, 2010). However, it is unknown as to whether or not the loss of Tpl-2 leads to higher incidence of skin tumors that have the potential to become invasive.

Unlike other enzymes, matrix metalloproteinases are not detected well in western blot analysis (Snoek-van Beurden and Von den Hoff, 2005). MMPs irreversibly lose their tertiary structure when they are boiled, which is a key step in western blotting before a sample is loaded onto the polyacrylamide gel. Also, reducing agents like β -mercaptoethanol—which is used in western blotting to separate multimeric proteins—are not desirable when studying MMPs because they break the disulphide bonds of MMPs in an irreversible manner, leading to unpredictably varying migration characteristics of MMPs and TIMPs (Snoek-van Beurden and

Von den Hoff, 2005). Instead of western blot analysis, then, the enzymatic activities of MMPs and TIMPs are studied using zymography and reverse zymography, respectively.

As gelatinases, MMP-2 and MMP-9 prefer to degrade gelatin. Therefore, their enzymatic activity is detected using gelatin as the substrate in zymography. Also, keratinocytes secrete MMPs as a way to help break down the extracellular matrix; thus, cell culture supernatants (conditioned media) from plated cells are the samples used in zymography (Xue *et al.*, 2004). The cell culture supernatant samples electrophorese on a polyacrylamide gel containing sodium dodecyl sulfate (SDS), which denatures/linearizes the proteins and gelatin under a high-voltage current. This electric current in a running buffer allows the different MMPs to migrate at constant rates that are inversely related to their molecular weight. After migration, the gel is placed in renaturing buffer to allow the proteins to regain their tertiary structure and enzymatic activity and then placed in developing buffer to allow the protease/MMP to digest its substrate, gelatin. The gels are then stained with a blue stain and destained (with SimplyBlue SafeStain and de-ionized water, respectively), and the results are white bands on a blue gel. Thicker bands are an indication of higher MMP enzymatic activity (Snoek-van Beurden and Von den Hoff, 2005).

Since zymography measures MMP enzymatic activity after denaturation and renaturation, it measures the MMP activity of all MMPs present in the sample, including pro-enzymes (which are a higher molecular weight), MMPs of a particular family (like gelatinases), and inhibitors/protectors to MMPs bound to them like lipocalin-2. Pro-MMP-2 and pro-MMP-9 have some enzymatic activity, but active MMP-2 and MMP-9 are the players responsible for extracellular matrix degradation. Therefore, because higher expression of active MMP-2 and MMP-9 is associated with tumor invasiveness, these are the forms that will be of particular

focus. However, the zymogens are also studied because they do have some enzymatic activity, even though it is lower. Also, the MMP-9/lipocalin-2 complex has been associated independently with a poor patient prognosis in previous research, but lipocalin-2 only protects MMP-9 activity; the complex does not play a role in the degradation of the extracellular matrix and lipocalin-2 has not been shown to be important by itself (Lee *et al.*, 2008). Another point worth noting is that gelatin is a common substrate for MMPs, and as such MMP-1, MMP-8, and MMP-13 can also be detected in gelatin zymography, although their enzymatic activity in digesting and degrading gelatin is typically significantly less than that of MMP-2 and MMP-9.

Because Tpl-2 is a tumor suppressor gene in mouse skin, unstimulated Tpl-2^{+/+} and Tpl-2^{-/-} primary keratinocytes are not cancerous. Therefore, in order to simulate the effects of an *in vivo* model, stimulators of Tpl-2 and NF-κB1 such as 12-O-tetradecanoylphorbol-13-acetate (TPA) and H-Ras retrovirus infection (also known as a transduction) with a mutant copy of the H-Ras oncogene are used in *in vitro* experiments to show genotypic differences. TPA is a tumor promoter drug that activates the protein kinase C-alpha (PKCα) pathway. PKCα is a serine/threonine kinase and a member of the conventional/classical PKCs, activated in response to several different stimuli. When activated, PKCα translocates from the cytosol to specialized cellular compartments, activating cellular functions like proliferation, differentiation, motility, and inflammation (Nakashima, 2002). Upon activation from agonists like TPA, PKCα phosphorylates a variety of substrates including those associated with the MAPK/ERK cascade. Raf-1 (a MAP3K protein) becomes phosphorylated, and the phosphorylation cascade continues to MEK and ERK, which then translocates into the nucleus, phosphorylating and targeting molecules for cell growth and cell survival (Fig. 11).

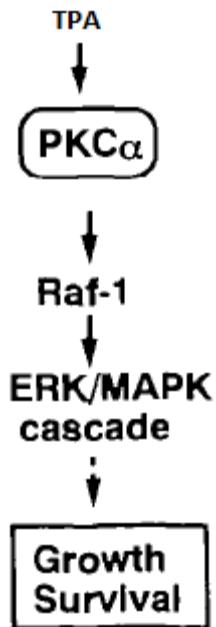


Figure 11: The Agonist TPA and its General Activation Cascade. The agonist TPA stimulates PKC α via phosphorylation, which activates/phosphorylates Raf (which are MAP3Ks), activating the ERK/MAPK cascade that ultimately leads to cellular growth and survival. Figure is modified from Nakashima, 2002.

TPA enhances the expression differences between Tpl-2^{+/+} and Tpl-2^{-/-} primary keratinocytes. Overexpression of PKC α promotes cellular proliferation and leads to a more aggressive phenotype involving tumorigenicity in some cell types. The activation of the MAPK/ERK cascade via PKC α facilitates the induction of cyclin-dependent kinase (CDK) to initiate the cell cycle (Nakashima, 2002). TPA also increases MMP-9 enzymatic activity and expression. MMP-9 induction via TPA is due to activated PKC α and the activated MAPK/NF- κ B1 pathways in treated cells, contributing to their migration and invasion if the cells have the potential to be tumorigenic and eventually metastatic (Lin *et al.*, 2009).

Additionally, TPA is used in *in vitro* experiments because it mimics the conditions used *in vivo* to generate skin tumor formation. In a two-stage skin carcinogenesis model, mouse skin is initiated with the carcinogen 7,12-dimethylbenz-(a)anthracene (DMBA), which causes point mutations in the Ras oncogene. TPA then promotes these Ras mutated skin cells to transform

into irreversibly-forming squamous carcinomas through chronic conditions of heightened inflammation. Skin tumors begin to arise after approximately 12 weeks depending on the strain of the mouse (DeCicco-Skinner *et al.*, 2010). Even though TPA alone is insufficient to promote skin tumor growth *in vivo*, it is used in *in vitro* models to mimic the inflammatory effects and epidermal hyperplasia seen *in vivo* (Furstenberger *et al.*, 1981).

H-Ras-infection involves the retrovirus infection of the mutant H-Ras oncogene. Cultured cells that have the H-Ras infection have stimulated Ras/Raf/Mek/Erk cascades. Considering that the mutant Ras oncogene is associated with approximately one third of all human cancers, H-Ras-infection is important to compare its effects between Tpl-2^{+/+} and Tpl-2^{-/-} keratinocytes. Skin tumors associated with a mutation in the Ras oncogene can be benign or malignant and can be precursor lesions to SCC. Thus, H-Ras-infection can show the potential for cells to transform into malignant and eventually metastatic ones after other genetic alterations, including mutations associated with the loss of Tpl-2 in mouse skin (Collard *et al.*, 1987).

An *in vitro* conversion assay is used to study genotypic differences in developing proliferative foci on cell culture plates. Foci are masses of cells growing on top of each other from cell colonies, indicative of normal cells converting into malignant ones. This conversion is difficult in primary cells like Tpl-2^{+/+} and Tpl-2^{-/-} keratinocytes without genetic alterations like mutated Ras, which is why H-Ras-infection is used in this experiment to aid in normal keratinocytes transforming into malignant ones. When constitutively-activated Ras is introduced to these primary keratinocytes in cell culture, a small proportion can convert into malignant keratinocytes and survive, while other keratinocytes that do not incorporate Ras will detach and undergo apoptosis (terminally differentiate) after calcium levels in media increase (Morgan *et*

al., 1992). After keratinocytes are plated, low calcium levels are used in the media for the first 2.5 weeks of the experiment to promote initial keratinocyte attachment as well as proliferation; high calcium levels in the media are then used for the duration of the experiment to stimulate cellular differentiation in keratinocytes that have constitutively active Ras. The formation of proliferative foci in media containing higher calcium concentrations can mimic the cellular and phenotypic changes seen for malignant conversion *in vivo* due to the mutated Ras oncogene. Cells in a few other plates are exposed to a known carcinogen, methylnitronitrosoguanidine (MNNG), which could provide a second hit to the already H-Ras-infected keratinocytes. Therefore, keratinocytes in these MNNG-treated plates are expected to convert faster than those cells that are only H-Ras-infected. This *in vitro* experiment involving cultured keratinocytes over the course of 12 weeks shows chemically induced focal neoplastic progression at the cellular level (Morgan *et al.*, 1992).

Another aspect of tumor invasion and metastasis is increased angiogenesis. There are *in vitro* and *in vivo* experiments to show differences between genotypes in potential angiogenic ability. In the *in vitro* assay, immortalized endothelial cells are plated on a gelled basement membrane (called matrigel) and form capillary-like structures/tubules based on the angiogenic factors from the conditioned media samples that the endothelial cells are plated with. The matrigel is a basement membrane extract obtained from a murine tumor that produces abundant extracellular matrix (Arnaoutova and Kleinman, 2010). The endothelial cells attach to the matrix, migrate toward one another, and form tubes over the course of 24 hours. The more nodes/tubules that are formed are indicative of higher angiogenic ability; these angiogenic differences are due to varying angiogenic factors from cell culture supernatant samples.

CHAPTER 2

OBJECTIVES AND SIGNIFICANCE

To assess whether keratinocytes from Tpl-2^{-/-} mice have the potential to have higher invasive and metastatic qualities than Tpl-2^{+/+} mice, I propose the following set of experiments.

Objective 1

To determine whether Tpl-2^{-/-} keratinocytes have elevated expression of MMP-2 and MMP-9 the following set of experiments will be conducted:

- (a) To identify differences in relative RNA expression of MMP-2 and MMP-9, microarray and qPCR will be performed.
- (b) To correlate gene expression differences with protein activity, zymograms will be conducted.

Objective 2

To determine if Tpl-2^{-/-} keratinocytes have increased migratory ability, malignant conversion, and conditions for angiogenic ability, the following will be performed:

- (a) Migration will be assessed through wound healing/scratch assays.
- (b) Potential metastatic characteristics will be analyzed through an *in vitro* conversion assay and a tubulogenesis assay.

CHAPTER 3

MATERIALS AND METHODS

Chemicals, Reagents, and Instruments

The following were used within this study: ethyl alcohol (Warner-Graham Company, Cockeysville, Maryland), Betadine (Express Medical Supply, Fenton, Missouri), Gibco® Dulbecco's Trypsin 0.25% (Invitrogen, Carlsbad, California), Dulbecco's Minimum Essential Medium (S-MEM—LoCa, 0.05mM Ca^{2+} and supplementing it with CaCl_2 to make HiCa, 1.3mM Ca^{2+}) (Lonza, Walkersville, Maryland), Falcon™ 100µM yellow cell strainer (BD Biosciences, San Jose, California), Centrifuge 5415R (Eppendorf AG, Hamburg, Germany), Dulbecco's Phosphate Buffered Saline (DPBS) (Invitrogen, Carlsbad, California), dimethyl sulfoxide (DMSO) (Thermo Scientific, Waltham, Massachusetts), collagenase (Worthington, Lakewood, New Jersey), fibronectin (BD Biosciences, San Jose, California), 12–0–tetradecanoylphorbol–13–acetate (TPA) (Alexis Chemicals, San Diego, California), MAP3K8 and Empty Vector virus (SAIC Frederick, Inc., Frederick, Maryland), Polybrene (Sigma, St. Louis, Missouri), Mitomycin C (Sigma-Aldrich®, Saint Louis, Missouri), Methylnitronitrosoguanidine (MNNG) (Sigma, St. Louis, Missouri), Zeiss Axiovert microscope (Thornwood, New York), Qiagen RNeasy® Kit (Hilden, Germany), RNase-free DNase (Qiagen, Hilden, Germany), GE NanoVue™ Spectrophotometer (Uppsala, Sweden), GeneChip Mouse Genome 430 2.0 arrays (Affymetrix, Santa Clara, California), GeneSpring 12.0 software (Agilent Technologies, Santa Clara, California), Pierce BCA Protein Assay Reagents A and B (Thermo Fisher, Rockford, Illinois), Multiskan FC microplate photometer (Thermo Fisher Scientific, Waltham, Massachusetts), Mammalian Protein Extraction Reagent (M-PER) (Thermo Scientific, Rockford, Illinois), Bovine serum albumin (BSA) (Sigma, St. Louis, Missouri), (10% Zymogram gelatin gels 1.0mm, 12-well (Invitrogen, Carlsbad, California), 10X Tris-Glycine SDS Running Buffer

(Invitrogen, Carlsbad, California), 10X Zymogram Renaturing Buffer (Invitrogen, Carlsbad, California), 10X Zymogram Developing Buffer (Invitrogen, Carlsbad, California), SimplyBlue™ SafeStain (Invitrogen, Carlsbad, California), Fisherbrand* 96-Well non-Skirted PCR Plate (Waltham, Massachusetts), Bio-Rad Optical Flat 8-Cap Strips (Hercules, California), SuperScript® III Platinum® SYBR® Green One-Step qPCR Kit w/ROX (Invitrogen™, Carlsbad, California), Invitrogen™ Custom DNA Oligos (Carlsbad, California), 24-well ImageLock™ plates (Essen Biosciences, Ann Arbor, Michigan), Essen Biosciences Wound Maker (Ann Arbor, Michigan), Essen Instruments IncuCyte Live Cell Imaging System (Ann Arbor, Michigan), Eppendorf *ep* Dualfilter *T.I.P.S.*® 0.1-10µL (Hamburg, Germany), Coulter Counter ZBI (Coulter Corporation, Hialeah, Florida), BD *Matrigel*™ Basement Membrane Matrix (BD Biosciences, Franklin Lakes, New Jersey), Gibco® Dulbecco's Modified Eagle Medium with 0.2% FBS with 100X Gibco® sodium pyruvate and *GlutaMAX*™ (Invitrogen, Carlsbad, California), and Dulbecco's Modified Eagle's Medium (D-MEM) (Lonza, Walkerville, Maryland).

Animals

Tpl-2 wildtype (Tpl-2^{+/+}) and knockout (Tpl-2^{-/-}) C57BL/6 mice were bred and maintained at the NIH animal facility, Building 28, in Bethesda, Maryland, following NIH animal guidelines. All animal work was performed following NIH guidelines under an approved animal protocol.

Newborn Mice Skin Removal

Since keratinocytes are believed to be the primary responder cell type of the skin, all *in vitro* experiments used primary keratinocytes as the main cultured cells.

To study genotypic differences between Tpl-2^{+/+} and Tpl-2^{-/-} mice for all of the experiments related to this thesis, primary keratinocytes were extracted from 1-3 day old newborn pups, following the protocol published by Lichti *et al.*, (2008). In brief, the pups were placed in a 150-mm plate (separate plates for separate genotypes), sacrificed by CO₂ asphyxiation for 30 minutes, and then dishes were placed in wet ice for an additional 30 minutes. The pups were then washed once with Betadine and twice with 70% ethanol, 30 seconds each. The tails and limbs were cut off, leaving a small stump to aid in the skinning process. The tails were saved for genotype confirmation and stored at -80 °C. A dorsal longitudinal incision was then created from tail to snout. The skins were removed and flattened with the dermis (shiny) side down, in a 150-mm dish and floated in 0.25% trypsin without ethylenediaminetetraacetic acid (EDTA)—which inhibits MMP enzymatic activity. The skins were then incubated overnight at 4°C.

Keratinocyte Preparation, Isolation, and Plating

The next day, the epidermises were carefully separated from the dermises using forceps and placed in a 50mL conical tube with approximately 15mL of HiCa media. Keratinocytes are sensitive to calcium levels. Thus, conditions for cellular differentiation require higher calcium levels (HiCa media) whereas normal feeding media for keratinocyte proliferation and attachment is at a lower concentration (LoCa media) (Lichti *et al.*, 2008). The epidermises were minced vigorously with scissors, pipetted up and down repeatedly and robustly for 1 minute (helping the keratinocytes separate from the strata cornea), filtered through a 100µM mesh cell strainer set in a 50mL conical tube, and centrifuged at 820-rpm at 4°C for 5 minutes. The media was aspirated, and the pelleted cells were then re-suspended in the corresponding amount of HiCa media, directly proportional to the original number of mouse skins.

Cells were plated fresh in 1:6 HiCa·LoCa media, which allowed for keratinocytes to attach to their substrate (the bottom of the wells) and grow; depending on the experiment they were plated by the following method: one mouse equivalent per 6-well plate, 2mL per well; two mouse equivalents per 24-well plate, 1mL per well (unless mentioned otherwise); or one mouse equivalent per 100-mm plate, 9-10mL per plate. Alternatively, keratinocytes could also be cryopreserved in 10% DMSO in liquid nitrogen. Cells that were formerly cryopreserved and restored were plated in 1:6 HiCa·LoCa media, one and a half mouse equivalents per 6-well plate, 2mL per well after each of the wells was coated with a collagen/fibronectin mixture with optional incubation period. The cells were incubated and allowed to grow overnight at 36°C in 7% CO₂. The media was changed the next day to LoCa media after the cells were checked for adequate growth and overall health. The media containing dead cells was aspirated, the cells were washed with DPBS and then aspirated, and LoCa media was added in the appropriate volume. Cells were then incubated overnight at 36°C in 7% CO₂. This protocol was used for all of the experiments relating to this thesis.

When cells were approximately 80% confluent (about 4-5 days after skinning), they were either left untreated, treated with TPA, H-Ras-infected, or MAP3K8-infected to compare genotypic differences.

TPA Treatment, H-Ras-transduction, Mitomycin C and MNNG Treatment, and MAP3K8 Overexpression

TPA stimulates keratinocytes through the PKC α pathway. To study genotypic differences, TPA treatment was given at different time points (18 hours, 4 hours, and 1 hour) at a concentration of 10ng/mL when the keratinocytes were 80% confluent. TPA comes in powder form and stocks (10mg/mL) were prepared in DMSO and stored at -20°C until ready for use. TPA treatment was used for the microarray, qPCR, and zymography experiments.

H-Ras-infection involves overexpression of the Ras oncogene via infecting the cells with a defective retrovirus containing the H-Ras oncogene, which constitutively activates its pathway. The H-Ras retrovirus is frozen and cryopreserved in liquid nitrogen until use, when it is then warmed in a 37°C water bath until thawed. It was then added in a 1:4 dilution in LoCa media with 4µg/mL Polybrene, which helps with infection efficacy. The H-Ras retrovirus contained 1 multiplicity of infection (MOI) in LoCa media. Old media was aspirated, 0.5mL of the virus was added to 1 well of a 6-well plate (350µL for a 24-well plate, 1mL for 60-mm dishes, or 2mL to 100-mm plates) for one hour. After 1 hour, 1.5mL of additional LoCa media was added in each well for a 6-well plate (150µL for a 24-well plate, 3mL for 60-mm dishes, or 8mL for 100-mm plates) and incubated for 24-72 hours at 36°C in 7% CO₂. Once finished, the media containing Ras was collected (in the case of zymography and the tubulogenesis assay) or removed and changed to fresh LoCa media. H-Ras-infection was used for zymography, the *in vitro* scratch assay, the *in vitro* conversion assay, and the *in vitro* tubulogenesis assay.

MAP3K8 overexpression temporarily restores MAP3K8 expression in Tpl-2^{-/-} keratinocytes for the *in vitro* scratch assay. Samples that were infected with the MAP3K8 adenovirus or empty vector adenovirus (a negative control) received 60 MOIs (multiplicity of infectious viral titers) per well of a 6-well plate containing approximately 700,000 cells (or 140,000 cells per well of a 24-well plate). 1mL of LoCa media for a 6-well plate (or 350µL for a 24-well plate) containing the virus was added for 1 hour. After the hour, 0.2mL of LoCa media was added in wells of a 6-well plate (150µL for a 24-well plate) and incubated and kept on the cells overnight. 60 MOIs is the standard for adenovirus infections. For adenovirus preparation, it was added into LoCa media with 4µg/mL Polybrene, and 1.2mL of the adenovirus was added to wells in a 6-well plate (or 350µL into wells of a 24-well plate) for 1 hour. After 1 hour, an

additional 200 μ L of fresh LoCa media was added to cells in a 6-well plate (150 μ L of LoCa for a 24-well plate) and incubated at 36°C in 7% CO₂ overnight. The media containing the adenovirus was aspirated and changed to fresh LoCa media the next day. MAP3K8 overexpression was used for the *in vitro* scratch assay with primary (non-H-Ras-infected) keratinocytes.

The antibiotic Mitomycin C inhibits cell replication, thereby allowing only migration differences to be compared between Tpl-2^{+/+} and Tpl-2^{-/-} primary keratinocytes for the *in vitro* scratch assay. Mitomycin C was prepared in deionized water and 1mg/mL stocks were stored at 4°C. Two hours prior to the start of the scratch assay, cells were treated with Mitomycin C at a concentration of 10 μ g/mL. Mitomycin C was only used in the *in vitro* scratch assay to inhibit cell replication such that only migratory differences could be compared between Tpl-2^{+/+} and Tpl-2^{-/-} keratinocytes.

MNNG is a known carcinogen used in the *in vitro* conversion assay because it provided a second ‘hit’ to aid in malignant cell conversion for 3 dishes from each genotype. Keratinocytes were treated with MNNG after H-Ras-infection and still in LoCa media. MNNG was prepared in ethanol at 0.2M. 25 μ L of stock MNNG was added to 25mL of LoCa media. 2mL of media containing MNNG was added to 3 dishes of 18 dishes per genotype (final concentration 20 μ M) for 1 hour and replaced by fresh LoCa media. The full protocol is described below.

RNA Extraction and Isolation

RNA extraction from Tpl-2^{+/+} and Tpl-2^{-/-} primary keratinocytes was used for microarray chip preparation and for real-time polymerase chain reaction experiments. RNA was extracted after primary keratinocytes were initially plated in the 1:6 HiCa:LoCa media and then changed to LoCa media the next day. Keratinocytes could then be left untreated or treated with 1 and 4 hours of TPA treatment before the RNA was extracted and isolated.

When ready, RNA was extracted, isolated, and purified from cultured primary keratinocytes using Qiagen spin columns according to manufacturer's instructions within the RNeasy kit. Samples were also DNase-treated on the column to remove any genomic DNA contamination. Pure RNA was resuspended in RNase-free ultrapure water. RNA concentrations were determined using the NanoVue Spectrophotometer and samples were stored at -80°C until use.

Affymetrix Microarray Preparation and Preliminary Data Filtering

A microarray experiment was performed to determine expression in the skin from Tpl-2^{+/+} and Tpl-2^{-/-} mice and to identify novel genes that are highly differentially regulated between genotypes when expression was compared. Twenty-four Affymetrix microarray chips were ordered for twenty-four RNA samples corresponding to two genotypes (Tpl-2^{+/+} and Tpl-2^{-/-}), three treatments (0 hour, 1 hour, and 4 hour TPA treatments), and four replicates. TPA treatment was used to mimic the heightened inflammation and epidermal hyperplasia observed in *in vivo* studies. RNA from five mice per genotype were prepared initially, and the four best replicates for each genotype and treatment were chosen for the experiment, based on RNA concentrations and QC reports performed by the National Cancer Institute in Frederick, MD. Five nanograms of RNA sample were sufficient for each chip array.

Each microarray chip for the twenty-four samples contains probesets (45,101 for GeneChip Mouse Genome 430 2.0 microarray chips), which measure mRNA expression. Each probe consists of a specific, target sequence for particular mRNA. Each probe also consists of a perfect match (PM) sequence and a mismatch (MM) sequence, which are adjacent to one another on the chip. The chosen sequence for each probe is determined by the 3' end of the transcript, which is unique and specific in the genome for each mRNA. The MAS5 (GCOS) algorithm was

used to transform the intensity on the chip to expression values used for analysis. MAS5 is the common normalization algorithm used for Affymetrix chips. It alleviates mismatch probes by obtaining a robust average for the PM and MM sequences for each probe. It also normalizes each of the arrays independently, assuming that the background noise on each chip may be different on other chips from the other samples.

GeneSpring 12.0 software was used for the microarray data analysis, and 45,101 features/probes were available for analysis initially. Each chip was median-centered, and all probes were then filtered such that intensity values needed to be above 50 for all 24 samples; otherwise, it was considered background noise and removed. The remaining 18,741 features were used for further analysis. The intensity values were then transformed using the binary logarithm (\log_2 -transformation) to normalize intensity values. Binary logarithm is common in computer scientific, mathematic, and information theory applications.

After log-transformation, the four array replicates for each experimental group were averaged, leaving two genotypes and three treatments, six groups total: 0 hour TPA treatment, 1 hour TPA treatment, and 4 hour TPA treatment for the two genotypes—Tpl-2^{+/+} and Tpl-2^{-/-}.

Zymography Preparation and Protocol

To measure MMP-2 and MMP-9 enzymatic activity, zymography using 10% Tris-Glycine gels containing 0.1% gelatin was used. Cell culture supernatants (the media from which the cultured cells were grown in that contain protein factors secreted from keratinocytes) were used for zymogram samples. These conditioned media samples were collected from keratinocytes that were untreated, H-Ras-infected, TPA treated for 18 hours, or both H-Ras-infected and TPA treated. Samples in 1.5-mL microcentrifuge tubes were spun at 13,200-rpm for 10 minutes to pellet and remove the excess cells in the media.

To measure the protein concentration of the cell culture supernatant, a BCA Protein Assay Kit was used (Thermo Fisher). The BCA protein assay uses a standard curve to determine protein concentration from the relationship between a sample's absorbance—the amount of color change and how much light can pass through the sample—and its total protein concentration. Samples were diluted 1:20 with Mammalian Protein Extraction Reagent (M-PER). Bovine serum albumin (BSA) served as a standard and was added to a 96-well plate in concentrations that ranged from 0 to 2mg/mL. The plate was incubated for 30 minutes at 37°C and then read on a MultiSkan FC plate reader at a wavelength of 570nm. Samples were compared to a standard curve.

18 micrograms of sample was loaded into each well of the gelatin gel, along with 2X loading buffer. Serum-free media was used to bring the total volume of each sample to 12 μ L. Loading buffer did not contain β -mercaptoethanol, which interferes with MMP activity. The gel was placed in running buffer with SDS (which linearizes/denatures the proteins). The gel was electrophoresed by applying 125 volts for 90 minutes in Tris-Glycine/SDS running buffer to provide a constant migration rate. Once finished, the gel cassette was cracked and the gels were placed in renaturing buffer within small boxes, shaking, for 30 minutes. The renaturing buffer quenches the SDS and allowed the MMPs to regain their tertiary structures and enzymatic activities. Next, the renaturing buffer was removed and developing solution was added for 30 minutes. After 30 minutes, fresh developing solution was placed on the zymogram gels overnight. This step allowed the MMPs and their complexes to digest the gelatin in the gel.

The next day, the gel was washed with deionized water three times for 10 minutes each, SimplyBlue SafeStain was added to the gel for 1 hour, the gel was destained with deionized water for 1 hour, and the gel was then ready to be photographed. The final gel was blue with

white bands corresponding to MMPs and their complexes. The thicker the white bands, the more concentrated the MMP protease was, representing higher enzymatic activity. A molecular weight protein marker (Sharp, Invitrogen Corporation) and MMP-2 and MMP-9 positive controls on each gel ensured correct identification of MMP-2 and MMP-9 bands. Densitometry with ImageJ software was used to compare band intensities between samples and all samples were normalized to the untreated Tpl-2^{+/+} sample to look at relative enzymatic activity.

Real-time Polymerase Chain Reaction (qPCR) Preparation and Protocol

Real-time polymerase chain reaction was used to determine MMP-2 and MMP-9 relative expression. The RNA samples that were used for the real-time polymerase chain reaction experiments were not the same as the samples from the microarray experiment because RNA collected for the microarray experiment were from individual mice; RNA samples for the real-time polymerase chain reaction experiments were collected from keratinocytes of several mice to ensure higher RNA concentrations. RNA was extracted and isolated from primary keratinocytes that were untreated, or treated with 1 or 4 hours of TPA. 100ng of RNA was loaded into each well of a 96-well plate. The qPCR reactions samples were prepared according to the manufacturer's instructions in a volume 50μL and triplicate wells containing 15μL each were used per sample. The reaction mix contained the following ingredients: 2μL of template RNA, 2μL of 10μM primer (with forward and reverse primers, final concentration 200nM), and 46μL of reaction mix in water. Unused RNA samples were stored at -80°C. The specific oligonucleotide primer sequences are provided:

Table 3: qPCR Primers for MMP-2, MMP-9, and β-actin

Primer	Forward Sequence	Reverse Sequence
MMP-2	CCTTAAAAGTATGGAGCGACGTCA	AGCGTTCCCATACTTTACGCG
MMP-9	ACCCTGTGTGTTCCCGTTCAT	GATACTGGATGCCGTCTATGTCGT

β-actin	TGGAATCCTGTGGCATCCATGAAAC	TAAAACGCAGCTCAGTAACAGTCCG
---------------------------------	---------------------------	---------------------------

Primer specificity was confirmed using Primer-BLAST; primers contained parts of the intron and exon. Each real-time PCR amplification cycle consisted of 95°C for 10 seconds and 60°C for 30 seconds for 50 cycles. β -actin served as the housekeeping gene.

In vitro Scratch/wound Healing Assay Preparation and Protocol

The *in vitro* scratch assay was used to visualize keratinocyte migration differences. Primary keratinocytes were isolated and plated in 1:6 HiCa:LoCa media and the media was changed to LoCa the following day. Keratinocytes were then grown until fully confluent in 24-well Essen *ImageLock* plates, where two mouse equivalents for each genotype (two mouse equivalents per 12 wells, 1mL per well) were initially plated. Some of the keratinocytes were H-Ras-infected to stimulate migration. Mitomycin C, which inhibits cell replication, was also added to respective wells at a final concentration of 10 μ g/mL two hours prior to the scratch. When ready, the bottom of the plate was scraped with a pipette tip to create a scratch/wound using the Wound Maker with four 0.1-10 μ L micropipette tips that simultaneously created precise and reproducible wounds in all wells of the plate, 4 wells at a time (Nelson *et al.*, 2010). The plate was then lined up with the A1 well in the Wound Maker, the tips were inserted onto the Wound Maker manually, the apparatus was placed down with the 4 tips in the first column and the plate was pushed gently back and forth. Resistance from the Wound Maker indicated when to stop moving the plate in one direction. In this way, the Wound Maker gently removed the cells from the confluent monolayer. A defined area of the scratch/wound could be visualized under a microscope at 10X magnification.

After scratching, the media was aspirated and washed twice in LoCa media to prevent dislodged cells from settling and reattaching. Once the wells were washed, 1mL of LoCa media

was added to each well and the plate was placed inside the IncuCyte™ system, which was stored in a 36°C incubator with 7% CO₂. The IncuCyte system photographed the scratch in each of the wells under phase-contrast microscopy every 4 hours, and measurements of the percent of wound closure were determined by the IncuCyte system. Scratch assays typically ran for 48 hours and plates were discarded after each run. The scratch assay looked at migration differences between genotypes when the keratinocytes were untreated, treated with Mitomycin C, H-Ras-infected, and H-Ras-infected as well as treated with Mitomycin C.

In vitro Conversion Assay Preparation and Protocol

To determine keratinocyte malignant conversion differences between genotypes, the *in vitro* conversion assay was prepared and run as described by Morgan *et al.* (1992). In brief, primary keratinocytes were isolated and plated in 1:6 HiCa:LoCa media and media were changed to LoCa the following day. 18 dishes were used for each genotype and keratinocytes were plated such that 0.3 mouse equivalents were plated in 60-mm plates in 3mL of media. The cells grew until they were 80% confluent, and all plates were H-Ras-infected in LoCa media for 48 hours. The media was then changed to fresh LoCa media. Four days after the removal of the H-Ras-infected media, 6 of the plates (3 dishes per genotype) were treated with MNNG, 20μM, for 1 hour and the media was then changed to LoCa media. MNNG treatment was used to provide a second ‘hit’ to aid in malignant conversion. Then, one week after H-Ras-infection and 4 days after 3 dishes per genotype were treated with MNNG, cells from one MNNG-treated plate for each genotype were trypsinized and counted using the Coulter Counter. This was done to determine cell loss due to carcinogen treatment. Keratinocytes grew in LoCa media until one week after the MNNG treatment (2.5 weeks into the experiment), when the media in all of the

remaining dishes was changed to HiCa media for the duration of the experiment, changing the media to fresh HiCa media twice a week.

Plate contamination did not start until 8 weeks into the experiment, which included 3 plates: two Tpl-2^{-/-} plates and one Tpl-2^{+/+} plate that was MNNG-treated. These dishes were fixed and stained with rhodamine in 10% formalin, which helped identify proliferative foci, clustered cells that stained a darker pink in a light pink to clear background, which are a sign of cellular malignant conversion. Rhodamine stains the actin in the cells, and formalin fixes cells by cross-linking proteins. At 12 weeks, the rest of the keratinocytes in the remaining dishes were stained with rhodamine and fixed in 10% formalin such that the numbers of foci were tallied for each genotype and compared.

In vitro Angiogenesis/tubulogenesis Assay Preparation and Protocol

An *in vitro* tubulogenesis assay was carried out to examine potential angiogenic ability. The assay requires a gel basement-like membrane (matrigel), immortal 3B11 parental endothelial cells (grown in 37 °C with 5% CO₂), and cell culture supernatant samples. The conditioned media was collected from keratinocytes that were untreated or H-Ras-infected. The tubulogenesis protocol used is described by Arnaoutova and Kleinman (2010). Briefly explained, the day before the assay, the 3B11 endothelial cells were serum starved in DMEM with 0.2% fetal bovine serum (FBS). The matrigel is frozen until ready for use. The 24-well plate to be used for the assay and matrigel (once thawed) were kept on ice. Approximately 250μL of matrigel was added and dispersed evenly on each well, minimizing any bubble formation. The plate was then placed in a 37°C with 5% CO₂ incubator for 30 minutes. In the meantime, the endothelial cells were detached with 2mL of trypsin; 10mL of LoCa media was added to deactivate the trypsin; the cells were filtered with a 100μM cell strainer to prevent

cellular aggregates; and cell count was determined using a Coulter Counter. After 30 minutes, the matrigel solidified, forming a substrate that mimics the basement membrane of a cell. 300μL of cell culture supernatant—from Tpl-2^{-/-} and Tpl-2^{+/+} keratinocytes that were either untreated or H-Ras-infected—was mixed with 80,000 3B11 endothelial cells and layered on top of the matrigel (separate wells per treatment). The plate was placed in the 37°C with 5% CO₂ incubator overnight.

The next day, the endothelial cells were viewed under a Zeiss Axiovert microscope (10X objective) to look for tube formation from the endothelial cells, which depended on what angiogenic factors were secreted from keratinocytes in their conditioned media. The number of nodes was then compared between samples. More nodes/tubes that formed in a well were an indication of potential higher angiogenic ability of Tpl-2^{+/+} and Tpl-2^{-/-} keratinocytes.

Microarray Data Analysis

After filtering, binary log transformation, and array replicate mean-averaging, expression differences were compared. Heatmaps and tables of fold change expression were used. A heatmap was then created for MMP-2, MMP-3, MMP-9, the four TIMPs, and lipocalin-2. Tables of fold change differences were produced to show genes that were significantly up- or down-regulated based on genotypic differences. A fold change greater than 2 was considered significant. A fold change table that compared expression values of Tpl-2^{-/-} to Tpl-2^{+/+} was created using three fold change ratios for each of the three TPA treatments:

KO 0h/WT 0h

KO 1h/WT 1h

KO 4h/WT 4h

Heatmaps generated by GeneSpring showed up-regulation in red, down-regulation in blue, and no expression change in yellow. Brighter coloration corresponded to higher/lower regulation.

qPCR Data Analysis

MMP-2 and MMP-9 relative expression levels were determined with Ct values using the Pfaffl method as previously described in Pfaffl, 2001. Ct values were normalized with beta actin, and relative expression differences were calculated comparing relative expression differences between Tpl-2^{+/+} and Tpl-2^{-/-} samples. A sample calculation for relative expression of a wildtype sample is provided:

$$\text{Relative Expression WT} = 2^{([Ct(KO) - Ct(\text{beta actin})] - [Ct(WT) - Ct(\text{beta actin})])}$$

Relative expression was normalized to the relative expression of the Tpl-2^{+/+} sample with no TPA treatment. Relative expression was then graphed with standard deviation error bars calculated in Microsoft Excel. A two-sample t-test using experimental triplicates was used to determine level of significance.

Scratch Assay Data Analysis using IncuCyte

Percent wound closure measurements for each treatment were copied into Microsoft Excel, and graphs with standard deviation error bars were created for each treatment and genotype to show migratory genotypic differences when keratinocytes were untreated, treated with Mitomycin C (inhibiting cell replication), H-Ras-infected (stimulating keratinocyte migration), or H-Ras-infected while also treated with Mitomycin C.

In vitro Conversion Assay Data Analysis

The analysis involved identifying and tallying the number of proliferative foci and comparing between genotypes once the keratinocytes were stained with rhodamine and fixed in 10% formalin. Rhodamine stains the actin in the cells, and formalin fixes cells by cross-linking proteins. Conversion ability was also viewed by the total number of foci for each genotype compared to the number of experimental dishes, which served as replicates.

CHAPTER 4

RESULTS

The goal of Objective 1 was determining whether Tpl-2^{-/-} keratinocytes have elevated MMP-2 and MMP-9 expression and enzymatic activity.

Microarray

Global Results and Initial Filtering for Significant Gene Comparison between Genotypes Associated with TPA Treatment

The Affymetrix chips contain 45,101 probes, and this experiment consisted of 24 samples: two genotypes (Tpl-2^{+/+} and Tpl-2^{-/-}), three treatments (0 hour TPA, 1 hour TPA, and 4 hour TPA), and four replicates. TPA was used to mimic the inflammation and epidermal hyperplasia seen in *in vivo* studies (Furstenberger *et al.*, 1981). When the results from each of the chips were converted into intensity values, Affymetrix used their own algorithm for data normalization within each chip, MAS5, which converted expression seen on the chip into intensity values used for analysis in GeneSpring 12.0 software. These intensity values were median-centered and log-transformed (Fig. 12A).

Background noise on the chips was also considered. Before the data was median-centered and log-transformed, raw intensity values ranged from approximately 4 to 16,000; smaller intensity values suggest low/no expression. Affymetrix considers the possibility of background noise at low intensity values (around 50). Therefore, if a probe had low intensity values across all chip arrays (50 or below), the probe was considered irrelevant to this experiment and removed from the dataset. This filter was substantial, removing 26,360 probes and leaving 18,741 probes for further analysis. Experimental group replicates were then mean-averaged (Fig. 12B).

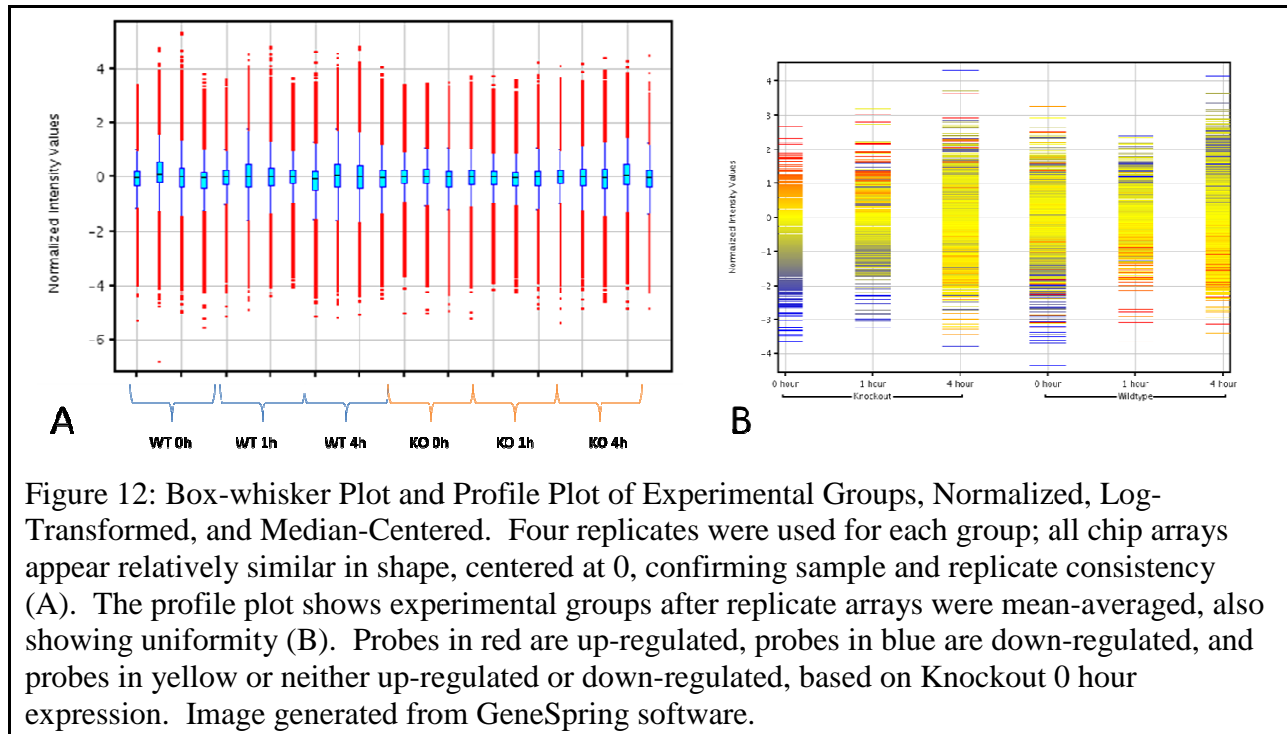
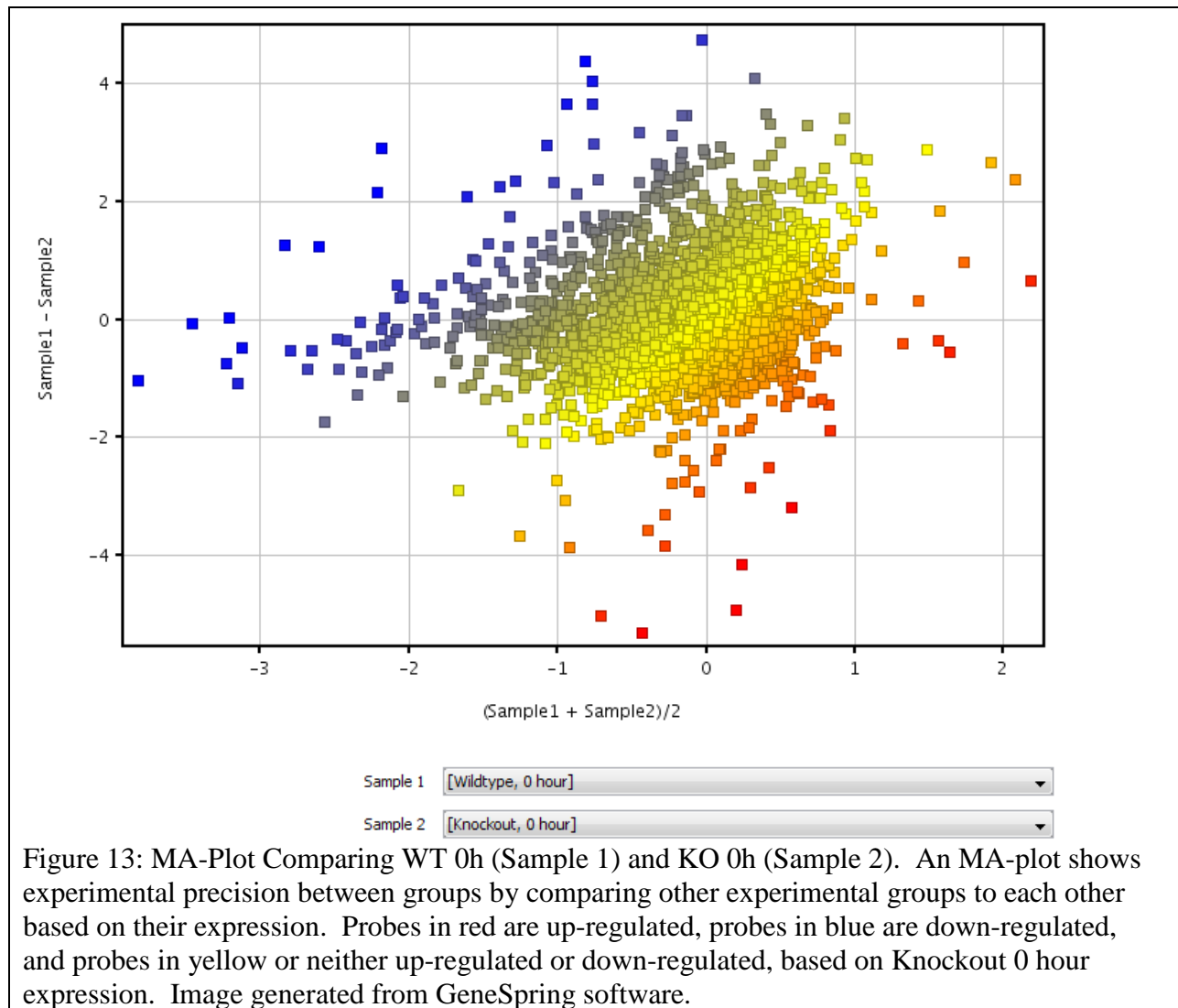


Figure 12: Box-whisker Plot and Profile Plot of Experimental Groups, Normalized, Log-Transformed, and Median-Centered. Four replicates were used for each group; all chip arrays appear relatively similar in shape, centered at 0, confirming sample and replicate consistency (A). The profile plot shows experimental groups after replicate arrays were mean-averaged, also showing uniformity (B). Probes in red are up-regulated, probes in blue are down-regulated, and probes in yellow or neither up-regulated or down-regulated, based on Knockout 0 hour expression. Image generated from GeneSpring software.

After replicates were mean-averaged, an MA-plot was created between two of the experimental groups. An MA-plot is a graphical way to compare normalized gene expression between two groups in single channel arrays like that of the Affymetrix chips used for this experiment. In the graph, log differences of two samples are plotted on the y-axis against the values' average (Pevsner, 2009). In this way, the data is centered on the x-axis, conveying consistency between experimental groups, with more up-regulated or down-regulated genes off of the x-axis (Fig. 13). If the data was not consistent between the two groups, the values in the MA-plot would be curved or off the center of the x-axis.



The samples for this MA-plot are the two genotypes, KO (Tpl-2^{-/-}) and WT (Tpl-2^{+/+}) at basal level (0 hour TPA treatment). As can be seen, the data values are generally centered on the x-axis, suggesting data precision between experimental groups. The probes in blue are down-regulated genes, red probes show up-regulation, and yellow probes are neither down- or up-regulated in respect to Knockout 0 hour samples. Other MA-plots that compare other experimental groups also have the same shape.

The remaining data could be filtered further. On a global scale, the data is compared using fold change ratios corresponding to effects between genotypes with TPA treatment consideration.

Fold change analysis compared expression between genotypes, Tpl-2^{+/+} and Tpl-2^{-/-}, with the same TPA treatments. Fold change expression was calculated using the following ratios:

KO 0h/WT 0h

KO 1h /WT 1h

KO 4h/WT 4h

If a probe had a fold change of two or higher (up- or down-regulated) for at least one of the three ratios, it was kept in the dataset; any probe that did not have a fold change of two or higher was removed. Differential regulation of a fold change of two or higher was chosen based on general acceptance in literature. However, there is a caveat when choosing how much fold change difference is necessary to be considered significant for a dataset because with this filter, a gene that may not be important to the study at hand could be kept, while another gene whose fold change values are close to 2 but do not make the cutoff is removed.

A heatmap was then generated from the remaining 1,097 genes/probes (Fig. 14). Genes were clustered such that those that were more similar in expression across experimental groups were clustered together on the heatmap. A dendrogram also showed gene expression relatedness. The experimental groups were also clustered using unsupervised hierarchical clustering based on centroid distance, related to the shared expression of experimental groups based on fold change from the three ratios that corresponded to genotypic differences. As can be seen, the genotypes share similar expression with each other and therefore are clustered together.

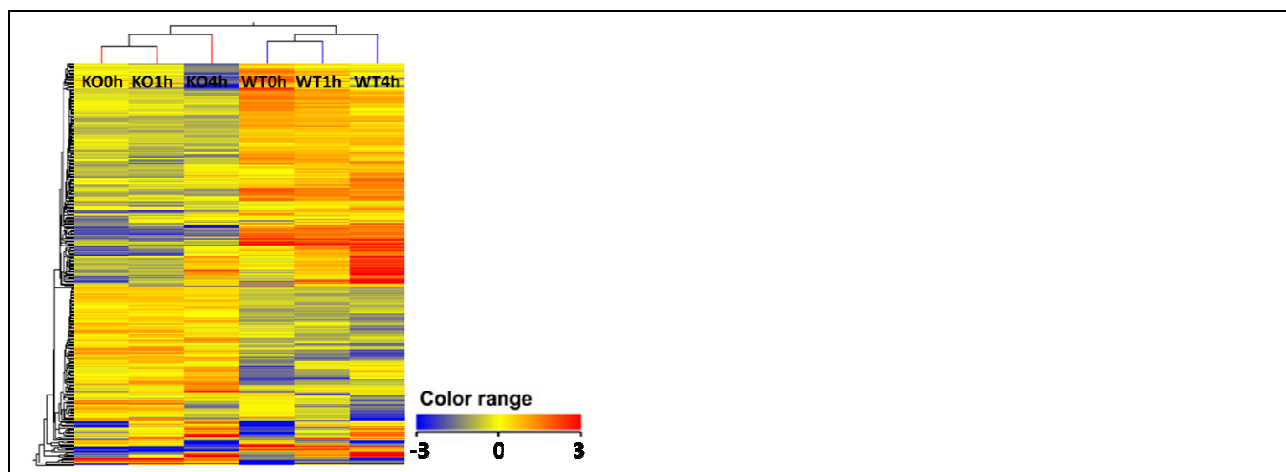


Figure 14: Global Heatmap of Differential Expression between Genotypes using Fold Change Filter 2 for the Three Ratios that Compared Expression between Genotypes across TPA Treatments. The genes are clustered by similarity across experimental groups. A dendrogram shows gene expression relatedness. Experimental groups are clustered using unsupervised hierarchical clustering from shared expression. Based on log-transformation and median-centering, genes in blue are down-regulated, genes in red are up-regulated, and genes in yellow are neither down- or up-regulated. As is seen in the profile plot (Fig. 12B), most genes are within the range -3 and 3. However only a select few genes are not within this range and they appear as the brightest blue and red, respectively. Image generated from GeneSpring software.

MMP-2, MMP-3, MMP-9, Lipocalin-2, and TIMPs: MMP-9
is Up-regulated in $Tpl-2^{-/-}$ Samples, while TIMP-2 is
Down-regulated with TPA Treatment

Since this experiment focuses on the potential of keratinocytes from $Tpl-2^{-/-}$ mice to become metastatic, it is important to see how key genes associated with tumor invasion differ between genotypes and how this expression changes with TPA treatment. In particular, higher MMP-2 and MMP-9 activity correlates with higher metastasis in cancerous cell types; MMP-3 has been shown to play a protective role against metastasis; higher expression of the MMP-9/lipocalin-2 complex is an independent sign of poor patient prognosis; and TIMPs inhibit MMP enzymatic activity and are therefore protective against cell invasion (Bauvois, 2012; McCawley *et al.*, 2008; Lee *et al.*, 2008; Folgueras *et al.*, 2004). The heatmap below (Fig. 15) shows these genes of interest together without any fold change filtering yet genes are clustered by similar expression. 19 genes are present, including splice variants.

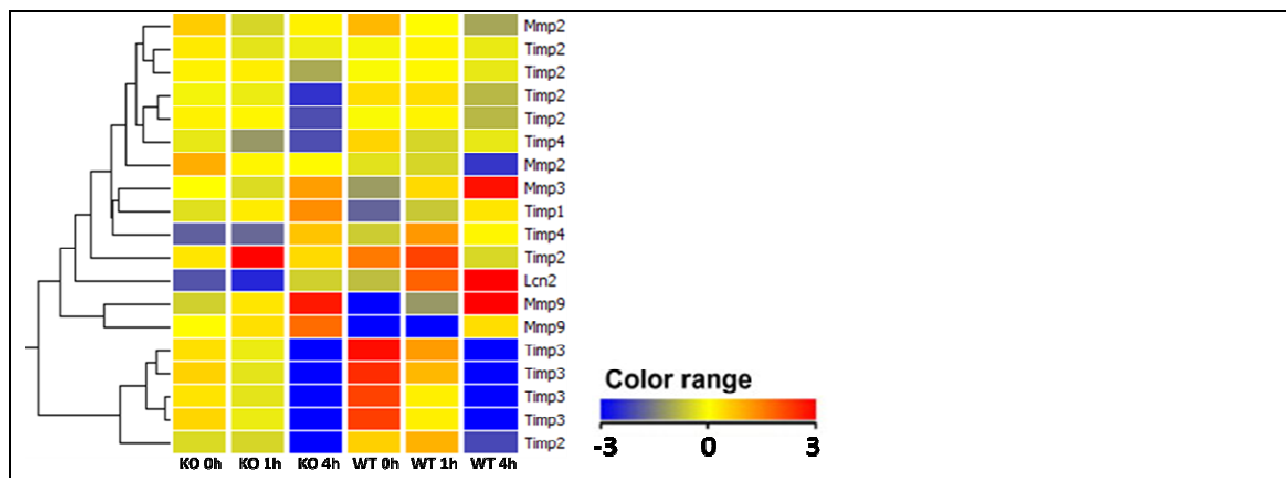


Figure 15: Heatmap of MMP-2, MMP-3, MMP-9, Lipocalin-2, and the TIMPs. The data is unfiltered, genes are clustered by similarity across experimental groups, and the dendrogram shows expression relatedness. Based on log-transformation and median-centering, genes in blue are down-regulated, genes in red are up-regulated, and genes in yellow are neither down- or up-regulated. Image generated from GeneSpring software.

These particular genes of interest and their splice variants were subsequently filtered using the ratios from above corresponding to expression differences between genotypes and how they compare with TPA treatment. Genes with that were differentially regulated by a fold change greater than 2 for any of the three ratios were considered significant and were kept in the dataset. The new heatmap shows these 5 significant genes that correspond to genotypic differences across TPA treatment (Fig. 16).

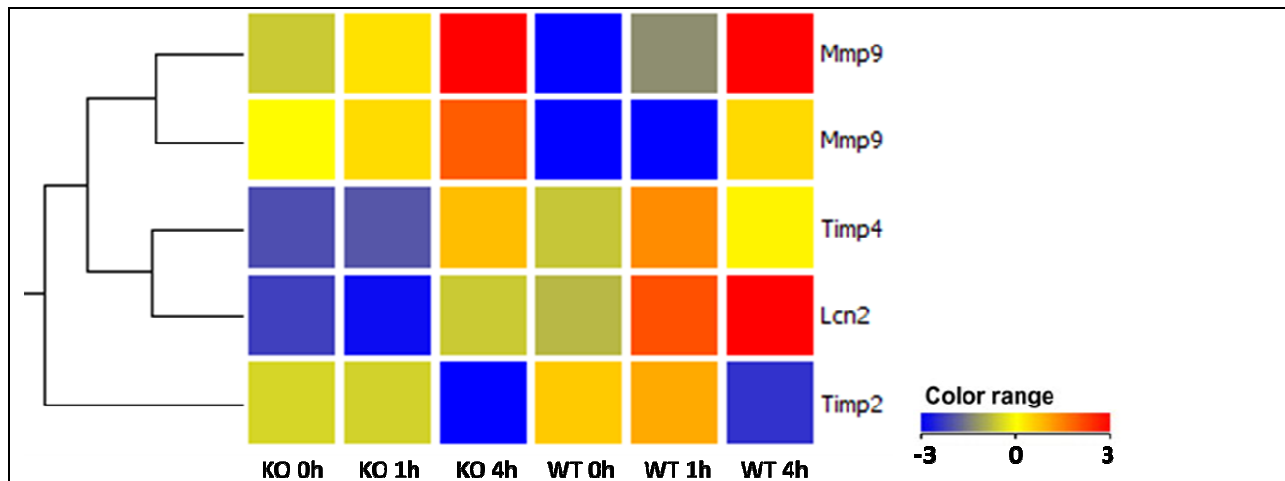


Figure 16: Heatmaps of Significant Genes based on Genotypic Differences from the 3 Fold Change Ratios for TPA Treatment. The original 19 genes were filtered down to 5 genes associated with genotypic differences compared across TPA treatment. Dendrograms show gene expression relatedness. Based on log-transformation and median-centering, genes in blue are down-regulated, genes in red are up-regulated, and genes in yellow are neither down- or up-regulated. Image generated from GeneSpring software.

Both splice variants of MMP-9 are up-regulated in $Tpl-2^{-/-}$ compared to $Tpl-2^{+/+}$ at basal level and are also up-regulated with TPA treatment, consistent with previous studies showing MMP-9 activation via TPA stimulation (Lin *et al.*, 2009). Lipocalin-2 appears to be up-regulated in $Tpl-2^{+/+}$ and becomes more up-regulated with TPA treatment. However, its complex with MMP-9 is what is associated with aggressive skin cancer types, not the gene by itself. This

gene may have other associations with Tpl-2 other than its complex with MMP-9. TIMP-2 appears to become down-regulated with TPA treatment. Taken together, MMP-9 up-regulation and TIMP-2 down-regulation coincide with each other since TIMPs inhibit MMP activity. If TIMP-2 is down-regulated, it can allow for higher MMP-9 expression.

Table 4 presents fold change expression ratio values for the significant genes based on genotypic differences across TPA treatment. The significant fold change ratios are in bold. Both splice variants of MMP-9 are up-regulated at basal level in Tpl-2^{-/-}; however, they both show a decreasing trend with subsequent TPA treatment, while lipocalin-2 is down-regulated in Tpl-2^{-/-} for 1 and 4 hour TPA treatments. Previous studies have shown that TPA activates MMP-9, and as such, TPA may activate MMP-9 in Tpl-2^{+/+} to a greater degree than Tpl-2^{-/-}, which could explain this trend, especially considering that the heatmap shows MMP-9 up-regulation in both genotypes with subsequent TPA treatment. Longer TPA stimulation may be necessary to support this suggestion. Also, as mentioned before, lipocalin-2 alone may be associated with Tpl-2 in other pathways, but its complex with MMP-9 is what is associated with aggressive skin cancer types. The association between lipocalin-2 by itself and Tpl-2 should be examined further.

Table 4: Significant Genes based on Genotypic Differences

Gene	KO0/WT0	KO1/WT1	KO4/WT4
Mmp9	3.75 up	2.58 up	1.42 up
Mmp9	2.70 up	1.47 up	-1.13 down
Timp4	-1.39 down	-2.17 down	1.16 up
Timp2	-1.29 down	-1.42 down	-2.31 down
Lcn2	-1.39 down	-3.14 down	-3.04 down

Another point worth mentioning is how MMP-2 is not present in the list of significant genes due to genotypic differential expression. MMP-2 is expressed at low levels in both genotypes in the microarray; however, it is up-regulated by 1.86-fold in Tpl-2^{-/-} after 4 hours of

TPA treatment, which explains why it was not included in the list of genes that were differentially regulated by a fold change of 2 or higher. Also, there are other MMPs that may have significant fold change differences between genotypes, but we chose MMP-2 and MMP-9 to study for this thesis since their up-regulation is closely associated with cell aggressiveness and metastasis.

Real-time Polymerase Chain Reaction for MMP-2 and MMP-9

Real-time polymerase chain reaction is a way to confirm gene expression differences between genotypes seen in the microarray experiment between Tpl-2^{+/+} and Tpl-2^{-/-} in mouse skin. Since MMP-2 and MMP-9 are up-regulated in invasive cell types, it is also important to study their relative expression in Tpl-2^{+/+} and Tpl-2^{-/-} keratinocyte RNA in a qPCR experiment, when expression is normalized to the unstimulated (no TPA treatment) Tpl-2^{+/+} RNA sample. Shown below, the qPCR results show up-regulation of MMP-2 in Tpl-2^{-/-} at basal level that increases with subsequent TPA treatment (Fig. 17A). MMP-9 is also significantly up-regulated in Tpl-2^{-/-} (Fig. 17B). All t-test results are at the p< 0.01 level.

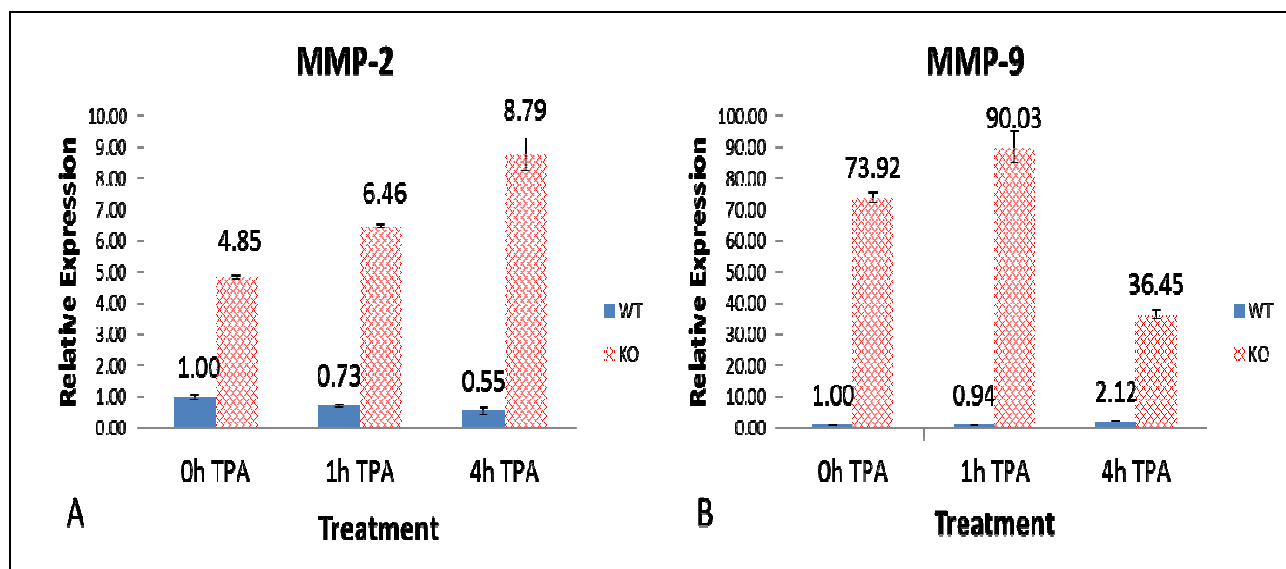


Figure 17: Real-time Polymerase Chain Reaction Results for MMP-2 (A) and MMP-9 (B). All expression is normalized to the Tpl-2^{+/+} sample that was not treated with TPA. MMP-2 is significantly up-regulated in Tpl-2^{-/-} and this up-regulation increases with subsequent TPA treatment, a similar trend that was seen in the microarray. MMP-9 is also significantly up-regulated in Tpl-2^{-/-}. Standard deviation error bars are also shown. All results are at the p< 0.01 level.

Zymography

Gelatin zymography detects MMP-2 and MMP-9 enzymatic activity due to their ability to digest gelatin, the denatured form of collagen. Zymography measures total enzymatic activity of MMP-2 and MMP-9, including active enzymes, pro-enzymes (zymogens), and MMP complexes with inhibitors and protectors like lipocalin-2 (Hu and Beeton, 2010). Cell culture supernatants (also called conditioned media samples) are the samples used in zymography because keratinocytes secrete MMPs into the media. Keratinocytes are isolated from pups 1-3 days old and plated in 1:6 HiCa:LoCa media, and the media are changed to LoCa the following day. Once the keratinocytes are 80% confluent, they were either untreated, H-Ras-infected, TPA treated overnight (approximately 18 hours), or H-Ras-infected and TPA treated, all of which was in LoCa media (Fig. 18). When ready, the conditioned media samples were collected and ready to be used for gelatin zymography, loading the same amount of sample in each lane. Shown below are the results for MMP-2 and MMP-9 total enzymatic activity.

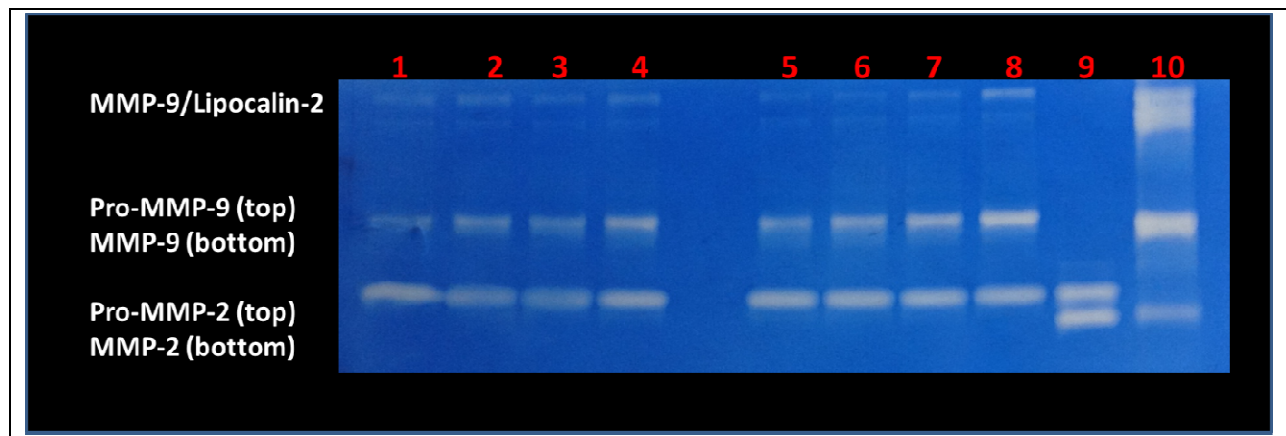


Figure 18: Gelatin Zymography with Untreated, H-Ras, TPA, and H-Ras and TPA Samples. Lane 1: WT Control; Lane 2: WT Ras; Lane 3: WT TPA; Lane 4: WT Ras+ TPA; Lane 5: KO Control; Lane 6: KO Ras; Lane 7: KO TPA; Lane 8: KO Ras+ TPA; Lane 9: MMP-2 positive control; Lane 10: MMP-9 positive control. Only bands corresponding to the MMP-9/lipocalin-2 complex and zymogens for MMP-2 and MMP-9 are present.

The band at 125-kDa is the MMP-9/lipocalin-2 complex; the band for pro-MMP-9 is at 92-kDa; the band for active MMP-9 is at 85-kDa; the band for pro-MMP-2 is at 72-kDa; and the band for active MMP-2 is at 65-kDa (Yan *et al.*, 2001). The highest enzymatic activity for the MMP-9/lipocalin-2 complex is from the Tpl-2^{-/-} H-Ras and TPA-treated sample. Also, pro-MMP-9 is higher in Tpl-2^{-/-}, especially in the TPA and Ras+ TPA samples. These results coincide with TPA treatment and MMP-9 activation (Lin *et al.*, 2009). The band corresponding to pro-MMP-2 is highest in Tpl-2^{-/-} samples. Densitometry was performed on this zymogram using ImageJ, where band intensities are normalized to the untreated Tpl-2^{+/+} conditioned media sample, and the results are presented below:

Table 5: Gelatin Zymography Densitometry Results

Sample	MMP-9/lipocalin-2	Pro-MMP-9	Pro-MMP-2
WT C	1.00	1.00	1.00
WT Ras	1.46	1.53	0.67
WT TPA	0.73	1.09	0.62
WT Ras + TPA	1.40	2.41	1.09
KO C	0.52	1.80	1.28
KO Ras	0.55	2.91	1.34
KO TPA	1.18	3.97	1.35
KO Ras + TPA	48.76	6.91	1.50

From the densitometry results, there are few enzymatic activity differences between samples corresponding to the MMP-9/lipocalin-2 complex, except for the KO Ras + TPA sample, which is dramatically higher than the rest of the samples. The band corresponding to pro-MMP-9 is higher in the Ras samples as well as the KO TPA sample, but the sample with the highest pro-MMP-9 enzymatic activity is the KO Ras + TPA sample. For pro-MMP-2, little

difference is detected, even though the Tpl-2^{-/-} samples are slightly higher in enzymatic activity than the Tpl-2^{+/+}. However, the difference is not as drastic as was seen in the samples relating to MMP-9, such as its zymogen and complex with lipocalin-2.

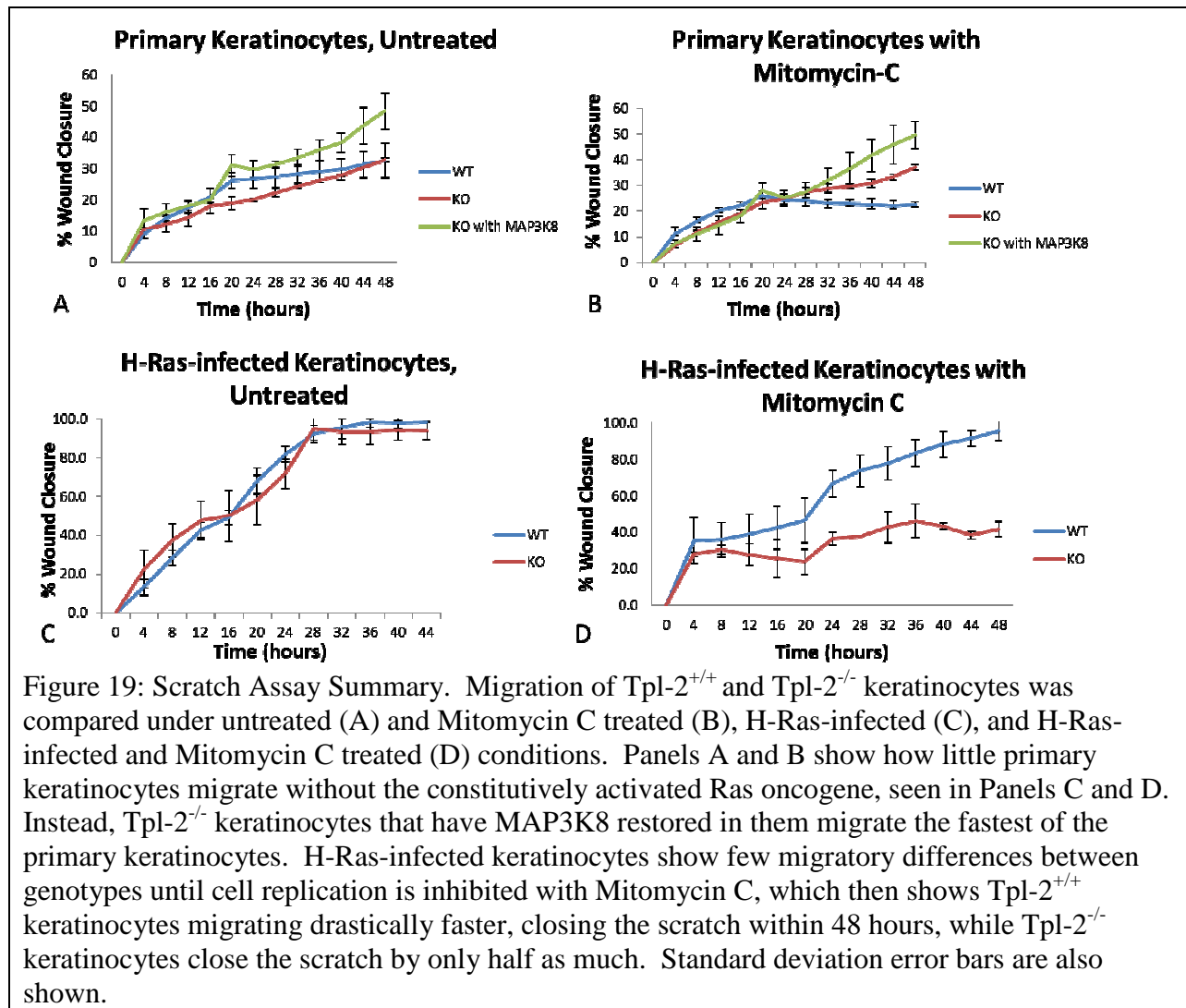
A point worth noting from the zymogram and from the densitometry results is the absence of active MMP-2 and MMP-9 bands. Their zymogens show enzymatic activity, but active MMPs are what are responsible for degrading the extracellular matrix in invasive cancers (Snoek-van Beurden and Von den Hoff, 2005). Pro-forms could be an indicator of how much active MMP activity is possible once MMP-2 and MMP-9 do become fully activated in aggressive cell types. Thus, from the results shown, Tpl-2^{-/-} samples, especially with the overexpression of the Ras oncogene and with TPA stimulation, have potential for high MMP-2 and MMP-9 enzymatic activity.

The goal of Objective 2 was determining if Tpl-2^{-/-} keratinocytes have the potential for increased migratory ability, higher malignant conversion, and better angiogenic ability.

In vitro Wound Healing/scratch Assay

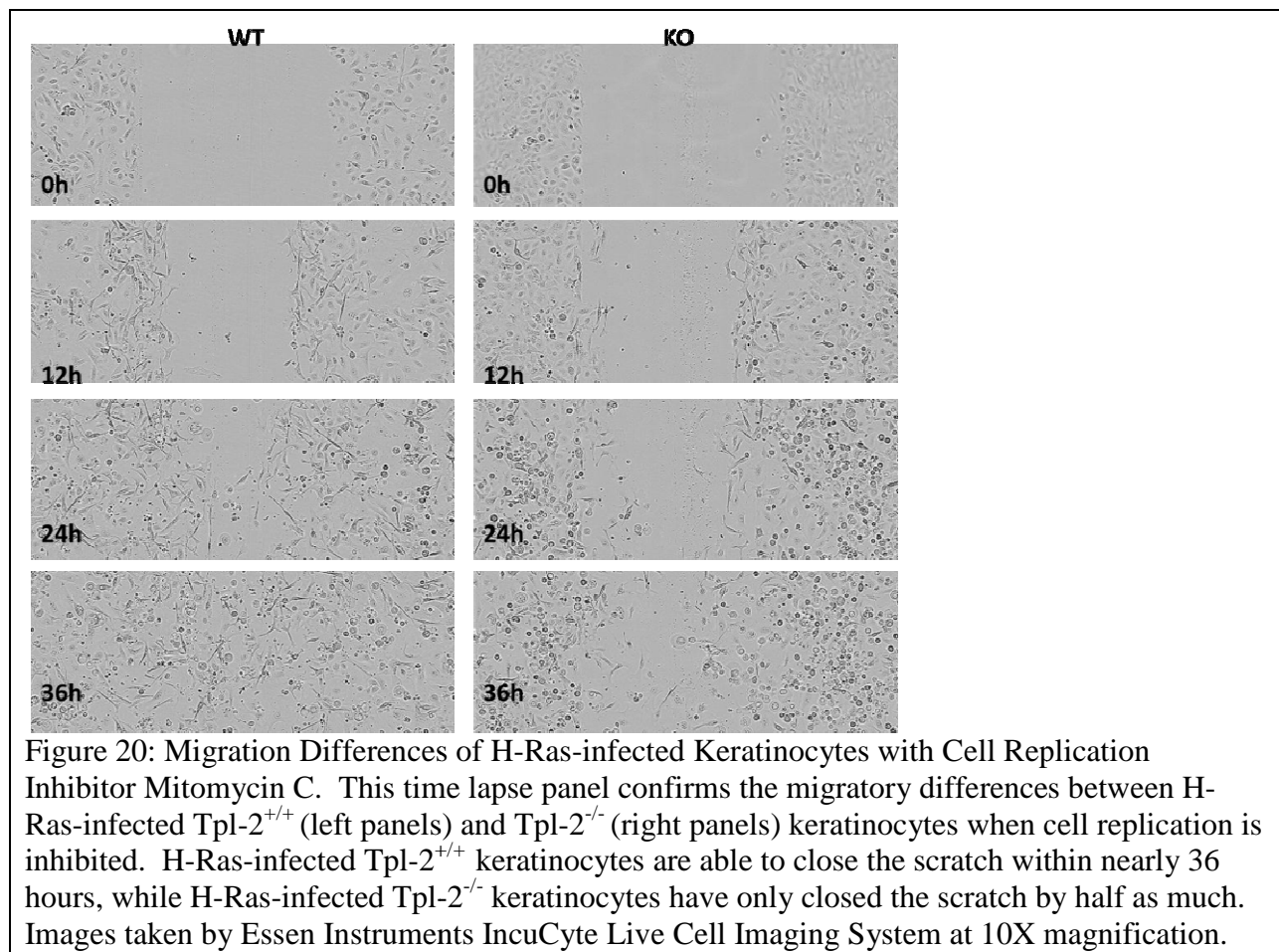
Scratch assays are a way of assessing cell migration rate. Using this assay, we compared migration differences in Tpl-2^{+/+} and Tpl-2^{-/-} keratinocytes while they migrated towards each other to close the scratch/wound. As previously described, keratinocytes were isolated and plated in 1:6 HiCa:LoCa media and the media was changed to LoCa media the following day. When the keratinocytes were confluent, they were either untreated, treated with Mitomycin C (which inhibits cell replication), H-Ras-infected, or H-Ras-infected and Mitomycin C treated (Fig. 19A-D). Some cells were H-Ras-infected, which constitutively activates the Ras oncogene and stimulates migratory pathways (Inamdar *et al.*, 2010). The antibiotic Mitomycin C was used

so that by inhibiting proliferation we can be sure that any wound closure is due strictly to cell movement and not due to an increase in cell number. The results of the scratch assay are presented below.



While there are few differences between primary Tpl-2^{+/+} and Tpl-2^{-/-} keratinocytes, Tpl-2^{-/-} keratinocytes migrate the fastest, however, when MAP3K8 is restored. These primary cells do not migrate quickly on the whole, though, since they are only able to close the scratch by less than 60% in 48 hours (Fig. 19A-B). H-Ras-infected Tpl-2^{+/+} and Tpl-2^{-/-} keratinocytes do not have different migratory rates. However, when cell replication is inhibited with Mitomycin C

treatment, H-Ras-infected Tpl-2^{+/+} keratinocytes migrate dramatically faster, closing the scratch in 48 hours, while Tpl-2^{-/-} keratinocytes have only closed the scratch by half as much (Fig. 19C-D and Fig. 20). Because Tpl-2^{-/-} H-Ras-infected keratinocytes migrate at the same rate as H-Ras-infected Tpl-2^{+/+} keratinocytes until their cell replication is inhibited, it could be suggested that Tpl-2^{-/-} H-Ras-infected keratinocytes have a faster cell cycle. However, this should be validated with other experiments.



The image shows that Tpl-2^{+/+} H-Ras-infected keratinocytes that are treated with the cell replication inhibitor, Mitomycin C, close the scratch more rapidly than H-Ras-infected Tpl-2^{-/-} keratinocytes. In fact, these Tpl-2^{+/+} keratinocytes are able to nearly close the wound within 36 hours, faster than any other sample and treatment.

In vitro Malignant Conversion Assay

The conversion assay compares the potential ability of Tpl-2^{+/+} and Tpl-2^{-/-} keratinocytes to convert into a malignant phenotype (i.e. form a pseudo-tumorlike state *in vitro*). This cellular conversion to malignancy could then later transform into aggressive and metastatic cell types. In this assay, keratinocytes are isolated and plated as previously described in 1:6 HiCa: LoCa media in 60-mm dishes, and the media are changed to LoCa the next day. To start, there were 18 experimental dishes per genotype, and 3 of these dishes were used for MNNG treatment. Once the keratinocytes are 80% confluent, they are infected with the Ras oncogene using a defective retrovirus in LoCa media. Those keratinocytes that do not take up the mutant Ras detach and undergo apoptosis when the media is changed (still in LoCa media), while the remaining H-Ras-infected keratinocytes continue to grow and proliferate. Then, 2.5 weeks into the experiment, the media is changed to HiCa media, which allows surviving H-Ras-infected keratinocytes to differentiate with potential for converting into malignant cells (Yuspa *et al.*, 1989). After 7-12 weeks (depending on mouse background), Tpl-2^{+/+} and Tpl-2^{-/-} dishes are stained with rhodamine in 10% formalin, looking for foci formation, which are the sign of cellular malignancy. Rhodamine stains the actin in the cells, and formalin fixes cells by cross-linking proteins. The more foci that form in the dishes, the better that genotype could be at potentially converting into malignant cell types. The results of the assay are presented below:

Table 6: Conversion Assay Results

Sample	Number of Foci after 12 Weeks	Conversion Ability
Tpl-2 ^{+/+}	0	0 of 15 plates
Tpl-2 ^{-/-}	7	7 of 15 plates

These results show a higher potential conversion rate for Tpl-2^{-/-} keratinocytes than Tpl-2^{+/+} keratinocytes when keratinocytes have the Ras oncogene constitutively activated.

The cells within the centers of foci on Tpl-2^{-/-} dishes also have cellular morphology unlike other keratinocytes that are not associated with foci (Fig. 21C). While normal cells exhibit contact inhibition and have normal keratinocyte morphology (Fig. 21A), the cells growing in the center of the focus show no contact inhibition (Fig. 21C), growing around and even on top of one another, characteristic of tumorous cells.

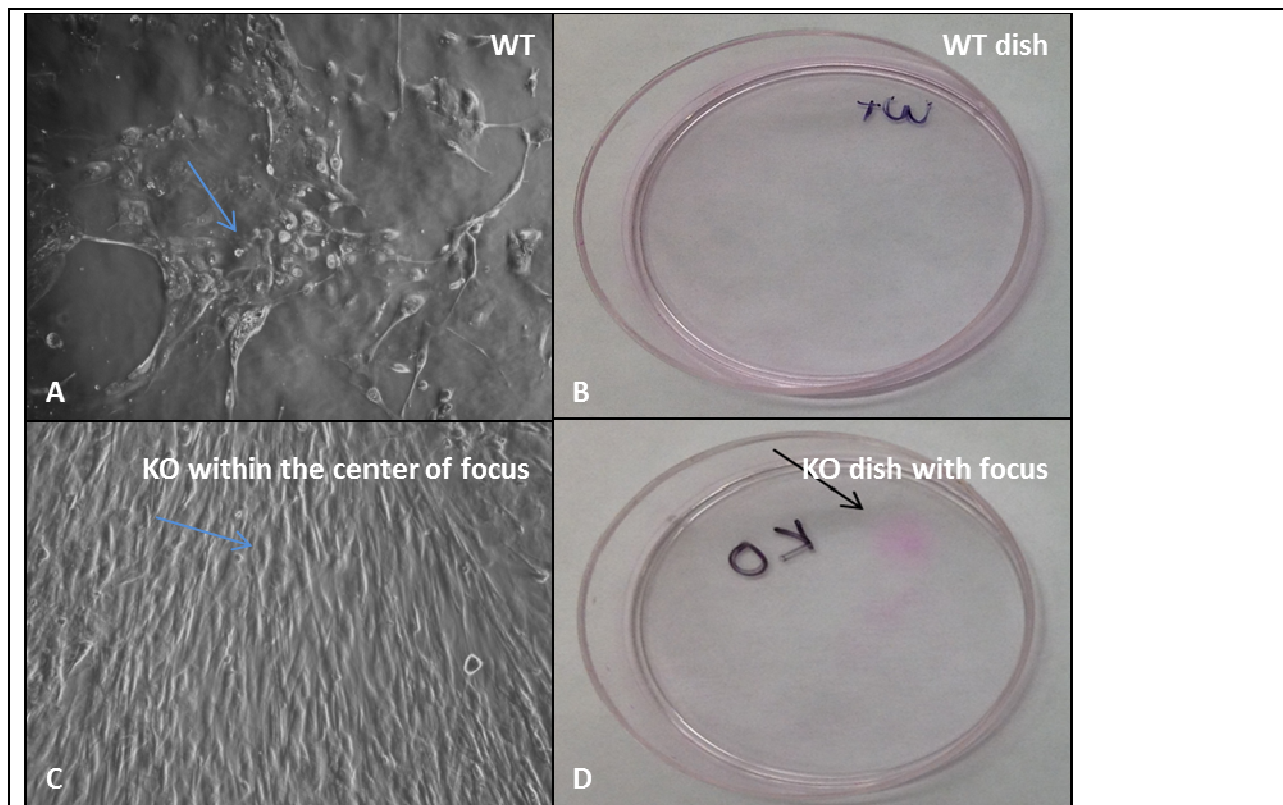


Figure 21: Keratinocyte Cellular Morphology and Conversion Assay Dishes after Rhodamine Staining. In dishes without any foci, which do not stain pink due to even cell dispersal in the dishes (B), Tpl-2^{+/+} keratinocytes are spread out evenly and exhibit contact inhibition (see the blue arrow in A). However, a Tpl-2^{-/-} dish with a focus growing in it stains as a spot of pink (black arrow in D), which are the converted cells growing within close proximity of one another. Under the microscope, these Tpl-2^{-/-} cells not only have different morphology than cells not associated with a focus, but they also exhibit no contact inhibition, growing on top of each other seen within the center of the focus (blue arrow in C). Images of the keratinocytes are taken from a Zeiss Axioplan II microscope at 5X magnification.

As is shown in the figure above, there are cellular morphology differences between cells that are seen in the center of the focus and cells that are not associated with a focus; they even stain differently. Keratinocytes that are not associated with a focus are not seen well with the

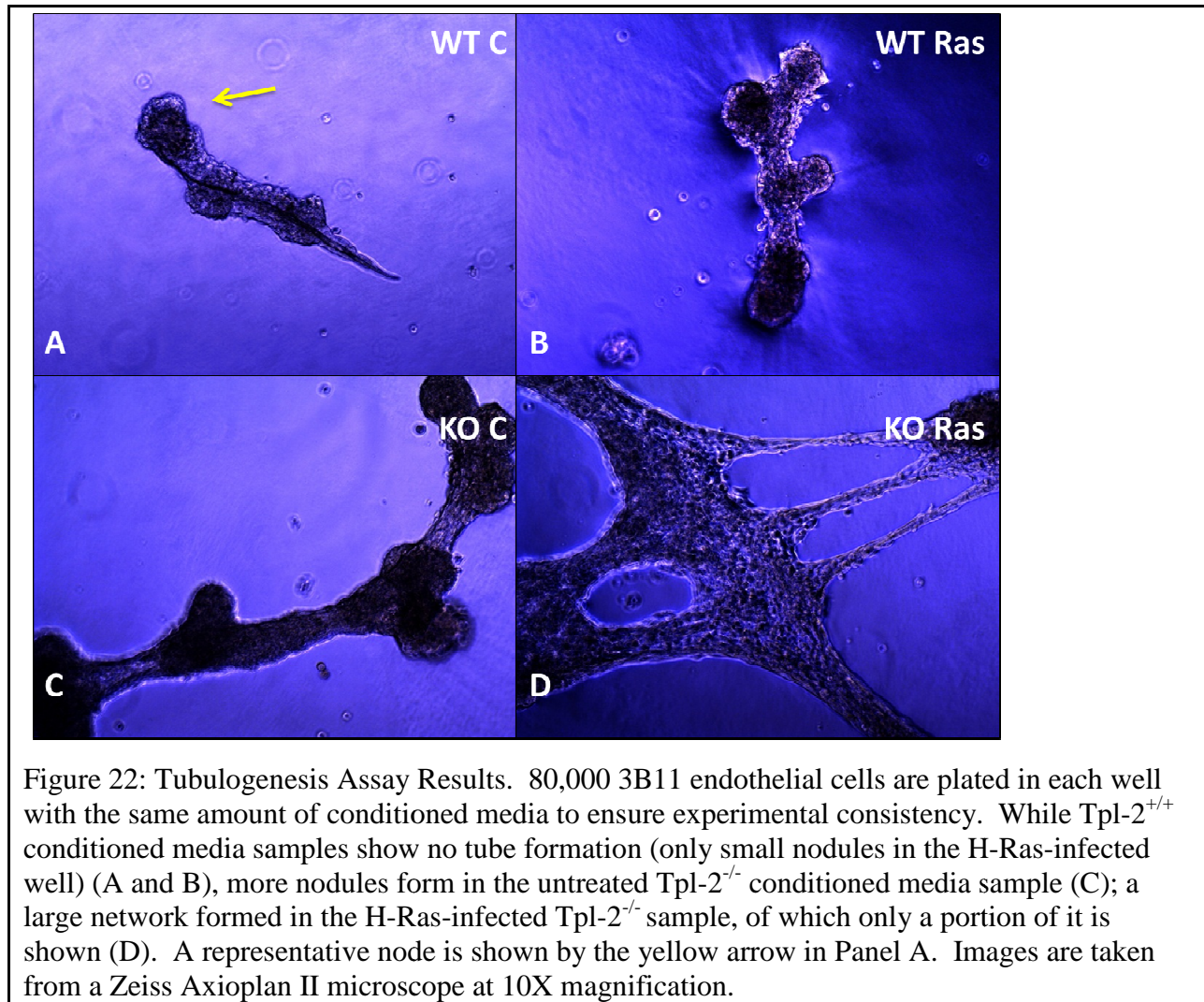
naked eye when they are stained with the pink dye rhodamine because they are dispersed evenly (Fig. 21B). However, a focus appears as a pink spot on the dish from the cells growing together in one area on Tpl-2^{-/-} dishes (Fig. 21D).

The results from the MNNG plates were not as expected. In addition to H-Ras-infection 3 dishes from each genotype were also treated with the carcinogen MNNG, which should have provided a second ‘hit’ to the cells that already have the Ras oncogene constitutively activated. Therefore, these dishes were thought to have had more foci form in them since they had additional genetic alterations (from treatment with the carcinogen) than those dishes that were only H-Ras-infected. Instead, however, no foci formed in dishes from either genotype.

In vitro Tubulogenesis Assay

The *in vitro* tubulogenesis assay shows the ability of cells to form tubes on a basement membrane, which can simulate potential angiogenic conditions *in vivo*. Immortal 3B11 endothelial cells (known for their high replicative ability) are plated with conditioned media samples and grow on a basement membrane-like gel. The same number of 3B11 cells is plated (80,000) to ensure consistency between samples. Keratinocytes from the conditioned media samples are isolated and plated in 1:6 HiCa:LoCa media and changed to LoCa media the next day. Once the cells are 80% confluent they are either untreated or H-Ras-infected, which can stimulate pathways associated with angiogenic factors (Ratushny *et al.*, 2012). The cell culture supernatant samples are collected because keratinocytes secrete angiogenic factors into the media. Thus, in this assay the more tubes that form in a sample are an implication of higher angiogenic ability based on the conditions that keratinocytes grow and survive in. This assay is important because higher angiogenesis is another characteristic of invasive and metastatic cell types (Masson *et al.*, 2005). As is shown in Figure 22, Tpl-2^{-/-} conditioned media samples enable

endothelial cells to form nodules and networks of tube formation in the matrigel more readily than Tpl-2^{+/+} conditioned media samples.



The figure above shows only a part of the network from the H-Ras-infected Tpl-2^{-/-} conditioned media sample. Figure 23, below, shows the full blood vessel network. These networks are from images taken by the microscope at 10X and pieced together to show the entire network, which is especially necessary for the H-Ras-infected conditioned media sample.

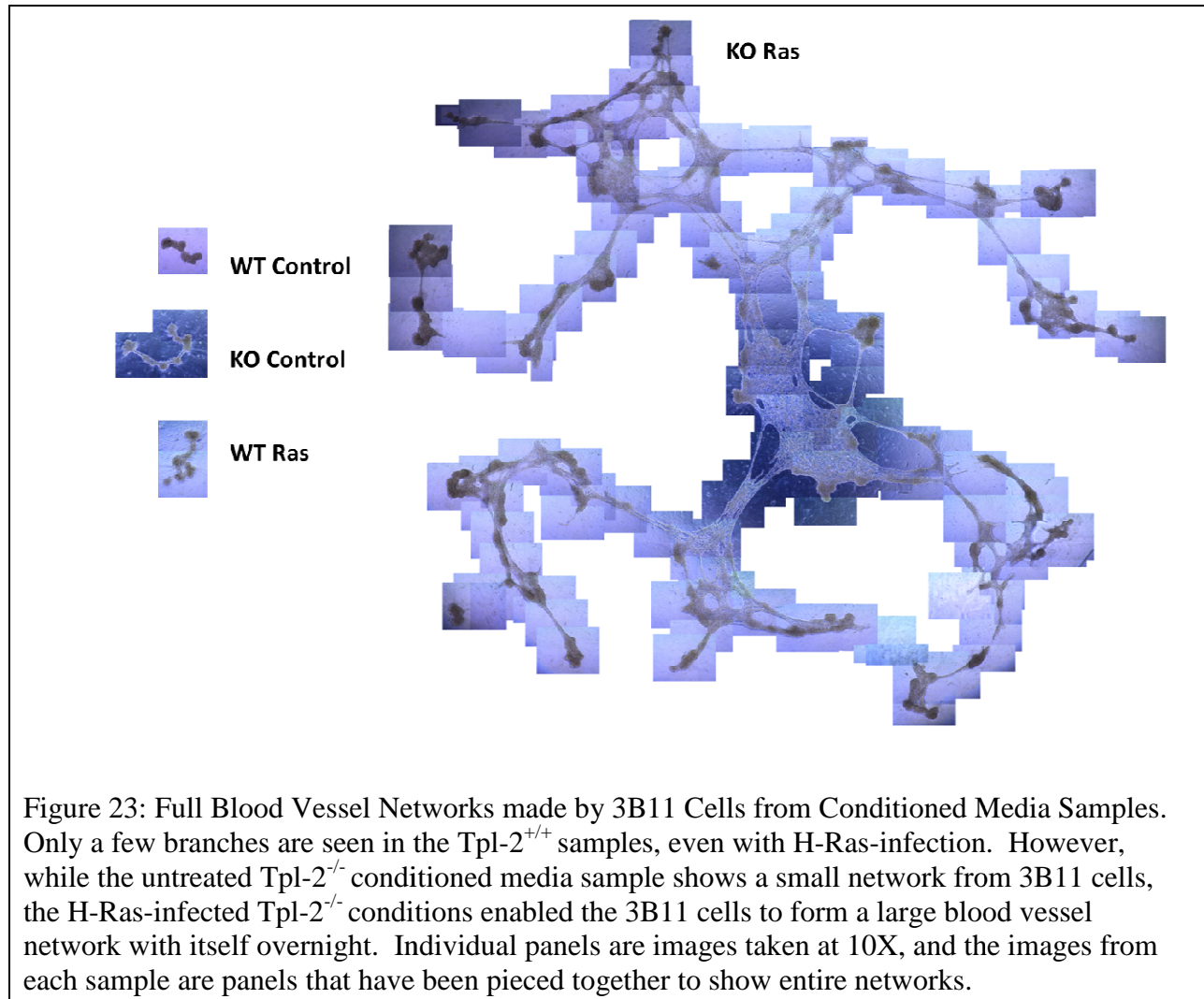


Figure 23: Full Blood Vessel Networks made by 3B11 Cells from Conditioned Media Samples. Only a few branches are seen in the $Tpl-2^{+/+}$ samples, even with H-Ras-infection. However, while the untreated $Tpl-2^{-/-}$ conditioned media sample shows a small network from 3B11 cells, the H-Ras-infected $Tpl-2^{-/-}$ conditions enabled the 3B11 cells to form a large blood vessel network with itself overnight. Individual panels are images taken at 10X, and the images from each sample are panels that have been pieced together to show entire networks.

The number of nodes/tubes that form in each of the samples was also tallied. As Figures 22 and 23 show, the 3B11 cells growing in $Tpl-2^{-/-}$ conditioned media show the potential for higher angiogenic ability than the cells in the $Tpl-2^{+/+}$ conditioned media. The quantitative data is presented:

Table 7: Quantitative Tubulogenesis Assay Results

Conditioned Media Sample	Number of Branch Sites
WT Control	3
WT Ras	5
KO Control	7
KO Ras	81

As is seen in Figures 22 and 23 as well as in Table 7, potential angiogenic ability is greater in Tpl-2^{-/-} conditions than in Tpl-2^{+/+} conditions, especially involving the Ras oncogene. When this assay is repeated this same trend is observed, but the numbers of tubes and nodes that form vary.

CHAPTER 5

DISCUSSION

Tpl-2 is a serine/threonine protein kinase that acts as a tumor suppressor in mouse skin. Its absence leads to NF- κ B1 and its downstream targets like Erk becoming constitutively active. This activation leads to a physiological response, such as chronic inflammation, that has been linked to the promotion of skin tumorigenesis due to constitutive activation. In previous research, it was found that Tpl-2^{-/-} mice have significantly more skin tumor formation and higher inflammation levels than Tpl-2^{+/+} mice (DeCicco-Skinner *et al.*, 2010). Both the increase in cell cycle and the inflammatory environment associated with this loss promote adequate conditions for skin tumorigenesis (Colotta *et al.*, 2009).

Even though Tpl2^{-/-} mice have a higher incidence of squamous skin tumor formation, it is unknown as to whether or not these tumors have potential for invasiveness and metastasis. Thus, this thesis studied the metastatic potential of Tpl2^{-/-} keratinocytes compared to keratinocytes from normal skin. Expression levels of MMP-2 and MMP-9 were considered since these MMPs in particular are associated with aggressive cell types as well as poor patient prognosis (Bauvois, 2012). Additionally, migration, malignant cell conversion, and angiogenesis were also examined considering that invasive cell types migrate faster, have higher malignant conversion, and are associated with enhanced induction of angiogenesis (Inamdar *et al.*, 2010; Morgan *et al.*, 1992; Masson *et al.*, 2005).

Genes Associated with Cellular Invasiveness like MMP-2 and MMP-9 are Up-regulated at the RNA Level in Tpl-2^{-/-} Mouse Keratinocytes

Matrix metalloproteinases degrade the basement membrane, which separates cells from underlying connective tissue and blood vessels. It has been well documented that invasive

cancerous cells have increased MMP activity, allowing them to enter the bloodstream and metastasize to other tissues (Folgueras *et al.*, 2004). The gelatinases MMP-2 and MMP-9 have been shown to play crucial roles in the ability of cancerous cells to invade and spread to other parts of the body. MMP-2 and MMP-9 can digest gelatin, which is the denatured form of collagen; thereby, they can aid in extracellular matrix degradation (Hu and Beeton, 2010). Consequently, MMP-2 and MMP-9 have been shown to be up-regulated in numerous cancer types, especially at malignant stages (Snoek-van Beurden and Von den Hoff, 2005). In these later cancerous stages, MMP-9 can influence cell behavior by activating major signaling pathways like NF- κ B and MAPK (Lin *et al.*, 2009). However, MMP-9 can also be stimulated by these same pathways in a positive feedback manner, thereby regulating pathways like cell growth, migration, invasion, inflammation, and angiogenesis and primarily causing the destruction of the extracellular matrix (Masson *et al.*, 2005).

The microarray, qPCR, and zymogram results show higher levels of MMP-9 in Tpl-2^{-/-} samples. The microarray results show higher MMP-9 expression at basal level of Tpl-2^{-/-} compared to Tpl-2^{+/+}, but both genotypes have up-regulated MMP-9 levels with subsequent TPA stimulation. TPA is known to activate MMP-9, which could account for the decrease in fold change results when comparing Tpl-2^{-/-} to Tpl-2^{+/+} MMP-9 expression with subsequent TPA treatment. However, qPCR results show significantly higher MMP-9 expression in Tpl-2^{-/-} RNA at basal level and with TPA. Taken together, MMP-9 up-regulation in Tpl-2^{-/-} is confirmed in both microarray and qPCR experiments.

The results from the zymogram show higher pro-MMP-9 levels in Tpl-2^{-/-} RNA, especially with TPA treatment and H-Ras infection. However, the band corresponding to active MMP-9 is not present, and active MMP-9 is responsible for degrading the extracellular matrix in

invasive cancers (Lin *et al.*, 2009). Pro-forms could be an indicator of how much active MMP activity is possible once MMP-9 is fully activated in aggressive cell types. Thus, from the results shown, Tpl-2^{-/-} samples, especially with the overexpression of the Ras oncogene and with TPA stimulation, have potential for high MMP-9 enzymatic activity.

Lipocalin-2 results, both from the microarray and from zymography where it is in a complex with MMP-9 are different than expected. Lipocalin-2 is down-regulated in the microarray with TPA treatment in the Tpl-2^{-/-} samples by 3-fold. Lipocalin-2 alone may be associated with Tpl-2 in other pathways, but its complex with MMP-9 is what is associated with aggressive skin cancer types, which could explain this discrepancy of why it is down-regulated in the Tpl-2^{-/-} especially after TPA treatment. In the zymogram, the MMP-9/lipocalin-2 complex is not drastically different between genotypes except for the conditioned media sample from TPA-treated and H-Ras infected Tpl-2^{-/-} keratinocytes, in which the densitometry results show an almost 50-fold increase between the TPA and Ras Tpl-2^{-/-} sample and Tpl-2^{+/+} control (untreated) sample. From these results, the association between lipocalin-2 and Tpl-2 should be examined further, especially considering that only the up-regulation of the MMP-9/lipocalin-2 complex is associated with several skin cancers (Lee *et al.*, 2008).

MMP-2 did not show up as a significant gene in the microarray data when comparing expression between genotypes with TPA treatment groups. However, MMP-2 is up-regulated in Tpl-2^{-/-} with 4 hours of TPA, but it was not included in the heatmap and table because it did not meet the fold change of 2 cutoff. This trend of increasing MMP-2 with TPA stimulation was also seen in the qPCR results such that MMP-2 was almost 10-fold higher in the 4 hour TPA Tpl-2^{-/-} RNA sample compared to the untreated Tpl-2^{+/+} RNA sample. MMP-2 relative

expression to untreated Tpl-2^{+/+} RNA was significantly higher in all of the Tpl-2^{-/-} samples, both untreated and treated with TPA.

Similar to the MMP-9 zymogram results, no active MMP-2 activity was detected but pro-MMP-2 activity was. However, from the densitometry results there were little differences in pro-MMP-2 activity from all of the conditioned media samples.

Tpl-2^{-/-} Keratinocytes May Migrate Slower when Cell Replication is
Inhibited, but their Higher Conversion Rate and Higher
Tube Formation with Mutated Ras Suggest
Potential for Aggressiveness and
Metastasis in Mouse Skin

Migration ability, malignant cell conversion rate, and angiogenic ability are all characteristics that can differentiate between normal and invasive cell types when taken together. Wound healing is a physiologically important process involving a multitude of proteins and molecules as well as cross-talk between pathways associated with cell proliferation, inflammation, and tissue repair (Werner and Grose, 2003). Keratinocytes are released from the basal lamina, whereby they dissolve the extracellular matrix via MMP proteolysis. However, in cancerous states cell proliferation, inflammatory, and tissue repair pathways become dysregulated. In the *in vitro* wound healing assay, an artificial gap (a scratch) is created on the confluent monolayer, and cells on the edge of the new gap migrate into the scratch until it closes. Some samples are treated with the replication inhibitor Mitomycin C, such that only migratory differences are observed, while other keratinocyte samples are not treated with Mitomycin C, allowing cell proliferation to be taken in consideration with migratory differences. In essence, the assay explores cell migration through interaction with the extracellular matrix *in vitro* (Nelson *et al.*, 2010).

In the scratch assay, Tpl-2^{+/+} keratinocytes migrated faster than Tpl-2^{-/-} keratinocytes when they were H-Ras-infected. While untreated keratinocytes migrated slowly, taking several days to close the scratch and showing little genotypic differences, Tpl-2^{-/-} keratinocytes whose MAP3K8 was restored migrated the fastest both with and without Mitomycin C treatment. When keratinocytes were H-Ras-infected with the Ras oncogene and treated with Mitomycin C, the migratory differences between genotypes were dramatically different. However, when these H-Ras-infected keratinocytes were not treated with the cell replication inhibitor, Tpl-2^{+/+} and Tpl-2^{-/-} keratinocytes migrated at the same rate and were able to close the scratch in 48 hours. From previous studies in other laboratories, it has been shown that Tpl-2 promotes cell migration mostly through ERK activation (Hatziapostolou *et al.*, 2011). Thus, it makes sense that Tpl-2^{+/+} keratinocytes migrate much faster than Tpl-2^{-/-} keratinocytes when cell replication is inhibited considering that Ras activates the MAPK/ERK pathways; without Tpl-2, the Tpl-2^{-/-} keratinocytes may use other migratory pathways. This clear difference in the results between H-Ras-infected keratinocytes that were treated with Mitomycin C and those that were not treated with Mitomycin C may also suggest that the tumors that form and may later metastasize due to the loss of Tpl-2 become invasive due to a faster cell cycle rather than because of migratory explanations.

Cell conversion is the ability of a cell to transform into a malignant cell type, which can later become invasive. Therefore, malignant conversion is an important characteristic to study when differentiating between aggressive and non-aggressive cell types and cancers. An *in vitro* conversion assay compared conversion differences between Tpl-2^{+/+} and Tpl-2^{-/-} keratinocytes that have the Ras oncogene constitutively activated by observing the development of foci formation (or lack thereof) on cell culture plates. Foci are an indication of normal cells

converting into malignant ones (Morgan *et al.*, 1992). This conversion will not occur in primary cells like Tpl-2^{+/+} and Tpl-2^{-/-} keratinocytes unless they acquire other mutations like Ras, which is why all surviving keratinocytes had the Ras oncogene constitutively activated. When the keratinocytes were infected with the Ras oncogene using a defective retrovirus, cells that did not incorporate Ras detached and terminally differentiated when media was changed from LoCa to HiCa after 2.5 weeks into the experiment. A small proportion of persisting cells that incorporated Ras could convert into malignant cells and produce proliferative foci. These malignant keratinocytes could then later transform into aggressive and metastatic cells. Thus, the production of proliferative foci can simulate the cellular and phenotypic changes seen in malignant conversion *in vivo* due to the mutated Ras oncogene as well as the absence of Tpl-2 in mouse skin (Morgan *et al.*, 1992). In this conversion assay, Tpl-2^{-/-} keratinocytes produced more foci than Tpl-2^{+/+} keratinocytes, which did not produce any foci in the experimental dishes. Thus, Tpl-2^{-/-} keratinocytes have better ability to convert to a malignant phenotype after Ras is mutated and constitutively activated.

Samples that received MNNG treatment did not work as planned. It was thought that the keratinocytes that were already H-Ras-infected could convert faster when given a second ‘hit’ from the carcinogen MNNG. Therefore, these dishes were thought to have had more foci form in them since they had additional genetic alterations (from treatment with the carcinogen) than those dishes that were only H-Ras-infected. 3 dishes from each genotype were treated with this carcinogen, and instead of forming more foci than the other experimental dishes, some of the Tpl-2^{+/+} dishes that received MNNG started to form foci, while only a few Tpl-2^{-/-} keratinocytes survived with the MNNG treatment. A cell viability assay may have been useful to determine if MNNG ended up being toxic to the Tpl-2^{-/-} and not Tpl-2^{+/+} keratinocytes. At the end of the

experiment and when all MNNG dishes were stained, though, no foci had actually formed in the Tpl-2^{+/+} dishes, and very few Tpl-2^{-/-} keratinocytes who received the MNNG treatment were able to survive.

Increased/sustained angiogenesis is another characteristic of aggressive cell types. In the *in vitro* tubulogenesis assay, immortal endothelial cells attach to the matrigel and migrate toward one another, forming tubes (similar to blood vessels) over 24 hours depending on their media conditions from the conditioned media samples that could contain varying angiogenic factors. The next day, the wells are viewed under the microscope; the more branches/tubes that form are indicative of conditions for higher angiogenic ability (Arnaoutova and Kleinman, 2010). These angiogenic differences are due to varying conditioned media from Tpl-2^{+/+} and Tpl-2^{-/-} keratinocytes. These cell culture supernatants will have different amounts of enzymes and growth factors, including varying MMP levels. MMPs have been shown to play a pivotal role in the formation of new blood vessels, especially in cancerous conditions (Folgueras *et al.*, 2004). From the experimental results, it is clear that Tpl-2^{-/-} conditions enable angiogenic ability better than Tpl-2^{+/+} conditions, especially in the H-Ras-infected conditioned media samples. Samples where keratinocytes were treated with TPA have yet to be tested, which could show promising results. However, especially considering the link between Tpl-2^{-/-} samples, MMP-9 up-regulation, higher conversion rates, and better angiogenic potential, it seems plausible that skin tumorigenesis due to the loss of Tpl-2 could have aggressive, invasive, and metastatic potential with other genetic mutations involved, such as the constitutive-activation of the Ras oncogene.

At basal level, there are genotypic differences between Tpl-2^{+/+} and Tpl-2^{-/-} samples, but loss of Tpl-2 does not seem to show a more aggressive phenotype without stimulating the primary keratinocytes through TPA treatment or H-Ras-infection. These results suggest that in

mouse skin, a number of genetic changes in addition to Tpl-2 loss are necessary for an aggressive cellular phenotype (Ratushny *et al.*, 2012). Thus, mouse skin cells that have lost Tpl-2 need other mutations or changes to occur before such invasiveness and metastasis. However, these results are important in linking malignancy and metastasis and the tumor suppressor Tpl-2 in mouse skin. These results potentially could be translatable to humans, associating the loss of MAP3K8 in human skin with having the potential to be aggressive and metastatic after other genetic alterations like the mutated Ras oncogene.

Future Experiments and Directions

There are many follow-up experiments and future directions that can be associated with these results. The experimental results from this thesis suggest that the skin tumors that form due to the loss of Tpl-2 in mice have the potential to be aggressive, invasive, and metastatic, even though other mutations and changes are necessary as well. Thus, there are many subsequent directions to explore this association at even greater depth.

This thesis focused on only a few MMPs that are associated with cell aggressiveness and metastasis: MMP-2 and MMP-9. However, there were other MMPs that were higher in Tpl-2^{-/-} samples than Tpl-2^{+/+} samples in the microarray. Using the three fold change ratios to compare genotypic differences across the three TPA treatments, Figure 24 shows the heatmap generated for these genes that were most differentially regulated, whose fold change was greater than 5 for at least one of the corresponding ratios, resulting in only 87 genes.

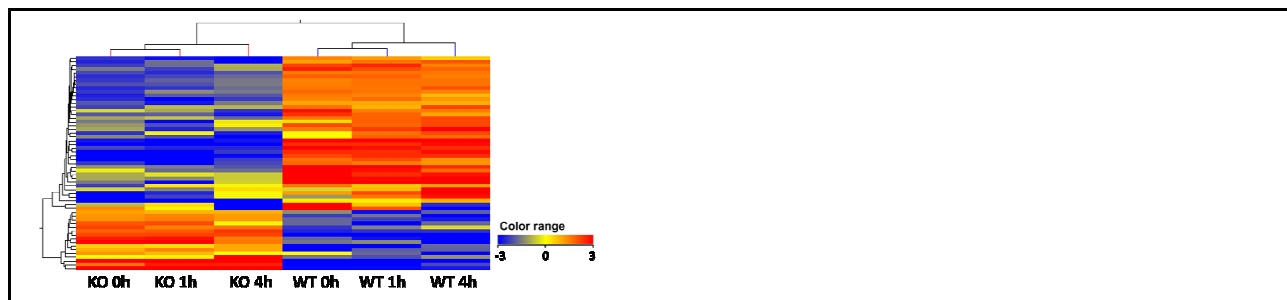


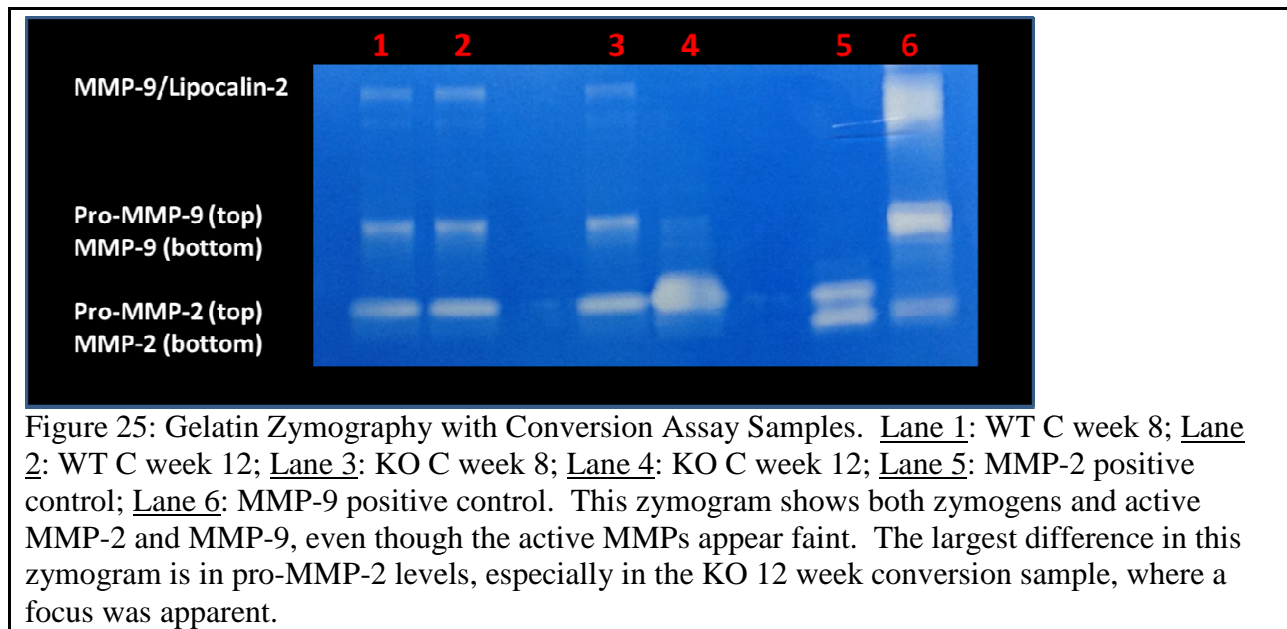
Figure 24: Heatmap with the Most Significant Genes Based on Genotypic Differences Across TPA Treatments. Genes in this heatmap had a fold change ratio of 5 or higher in at least one of the three fold change ratios that compared expression between genotypes. Genes more similar to each other across experimental groups are clustered together, and a dendrogram shows expression relatedness. Unsupervised hierarchical clustering grouped the experimental samples together that had shared expression. Based on log-transformation and median-centering, genes in blue are down-regulated, genes in red are up-regulated, and genes in yellow are neither down- or up-regulated. Image generated from GeneSpring software.

One MMP in particular that was included in this heatmap was MMP-1. It was up-regulated by over 7-fold in $Tpl-2^{-/-}$ at basal level compared to $Tpl-2^{+/+}$. Thus, MMP-1 may be important to study, especially if it relates to NF- κ B and MAPK pathways in relation to the loss of Tpl-2 in mouse skin.

Similarly, as was shown in the Results section, TIMP-2 and TIMP-4 were down-regulated in $Tpl-2^{-/-}$ samples by at least 2-fold. Since TIMPs inhibit MMP activity, the net balance between MMPs and TIMPs may be disrupted considering the TIMP down-regulation and MMP up-regulation, which is also responsible for the control of the degradation of the extracellular matrix (Folgueras *et al.*, 2004). Therefore, another experimental direction could be looking at the association between the loss of Tpl-2 in mouse keratinocytes and TIMP expression. Since they are a different family of enzymes than MMPs, detection of TIMP enzymatic activity would use reverse zymography or qPCR.

Another direction that shows promise from this thesis is the role of MMP-2 in cell malignant conversion. Even though MMP-2 was not found to be statistically different through microarray analysis, it was significantly up-regulated in RNA samples analyzed by qPCR. Additionally, we recently ran a zymogram using conditioned media samples from the *in vitro* conversion assay. We found that supernatants from $Tpl-2^{-/-}$ keratinocytes produced drastically higher MMP-2 enzymatic activity than supernatants from $Tpl-2^{+/+}$ cells despite the fact that total

protein levels were normalized between treatment groups (Fig. 25). Active MMP-2 and MMP-9 activity was also detected.



The results from this zymogram show little differences between cell culture supernatant samples from dishes without foci formation from both genotypes. However, the Tpl-2^{-/-} dish with the earliest-forming focus of the experiment has lower pro-MMP-9 and higher active MMP-9 activity as well as higher pro- and active MMP-2 activity. This sample is the first sample to reveal such stark MMP-2 differences as well as show active MMP-2 and MMP-9. The densitometry results from ImageJ are presented below.

Table 8: Conversion Gelatin Zymography Densitometry Results

Sample	MMP-9/lipocalin-2	Pro-MMP-9	Pro-MMP-2	MMP-9	MMP-2
WT C week 8	1.00	1.00	1.00	1.00	1.00
WT C week 12	1.40	1.10	1.42	3.83	2.46
KO C week 8	0.87	1.44	1.80	2.31	4.17
KO C week 12	0.10	0.23	3.76	53.05	5.81

The zymogram and densitometry results show bands for active MMP-2 and MMP-9, even though they are slight. The MMP-9/lipocalin-2 activity is higher in the Tpl-2^{+/+} samples, which may account for the higher pro- and active MMP-9 enzymatic activity. Active MMP-9

activity increased the longer the conversion assay continued, and by week 12, the Tpl-2^{-/-} conversion assay sample was much higher than the Tpl-2^{+/+} sample from week 8. Also, both pro-MMP-2 and MMP-2 are higher in the Tpl-2^{-/-} samples, especially after the focus formed in the dish (after week 8). Therefore, it is worth examining the association between MMP-2 and cellular malignancy related to the loss of Tpl-2 in mouse keratinocytes. Even though MMP-9 may be important in earlier skin cancer stages, MMP-2 may be a more important player at malignant and even later stages.

Yet another experimental direction could be examining some these genotypic differences seen in this thesis using an *in vivo* model. Both the scratch assay and tubulogenesis assay have *in vivo*-associated experiments. *In vivo* wound healing could be a great way to compare genotypic differences in the ability to close and fully heal a standardized and precise wound in mice. Similarly, the matrigel can be used with *in vivo* models by creating a plug on the backs of mice and comparing tube formation between Tpl-2^{-/-} and Tpl-2^{+/+} mice. The *in vivo* and *in vitro* tubulogenesis assays could also study VEGF content in cell culture media to support genotypic differences in potential angiogenic ability.

CHAPTER 6

CONCLUSIONS

Skin cancer is the most prevalent cancer in the United States; as such, it is important to examine mutations and changes involved that lead to tumorigenesis, cell malignancy, and metastasis. The purpose of my thesis was to study the aggressive, invasive, and metastatic potential of squamous skin tumors associated with the loss of Tpl-2 in mice. Previous research has shown that while Tpl-2 is seen as an oncogene in numerous cancer types—where its overexpression has been linked to breast cancer, lung cancer, prostate cancer, and some lymphomas—its absence has been shown to increase tumorigenicity in mouse skin. The results from my thesis revealed that these skin tumors may also have metastatic potential with other genetic alterations, such as mutant Ras. Upon stimulation with TPA or infection with the Ras oncogene (which frequently is mutated during skin tumorigenesis), Tpl-2^{-/-} keratinocytes have higher MMP-9 expression at the RNA level, a possible faster cell cycle, higher malignancy conversion rates, and more potential angiogenic conditions than Tpl-2^{+/+} keratinocytes. Taken together, the skin tumors associated with the loss of Tpl-2 have the potential to become invasive. However, like other tumor suppressors, other mutations and genetic changes are necessary before this metastatic potential is realized.

REFERENCES

2010. A Snapshot of Melanoma. National Cancer Institute. Last viewed March 2011. <www.cancer.gov>
2010. What You Need to Know about Melanoma and Other Skin Cancers. National Cancer Institute. Last viewed April 2012. <www.cancer.gov>
- Arnaoutova, Irina and Hynda K. Kleinman. 2010. *In vitro* angiogenesis: endothelial cell tube formation on gelled basement membrane extract. *Nature Protocols*. 5, 628-635.
- Bauvois, Brigitte. 2012. New facets of matrix metalloproteinases MMP-2 and MMP-9 as cell surface transducers: Outside-in signaling and relationship to tumor progression. *Biochimica et Biophysica Acta*. 1825, 29-36.
- Ceci, Jeffrey D., Christos P. Patriotis, Christos Tsatsanis, Antonios M. Makris, Robert Kovatch, Deborah A. Swing, Nancy A. Jenkins, Philip N. Tsichlis, and Neal G. Copeland. 1997. Tpl-2 is an oncogenic kinase that is activated by carboxy-terminal truncation. *Genes and Development*. 11, 688-700.
- Collard, John G., Jack F. Schijven, and Ed Roos. 1987. Invasive and Metastatic Potential Induced by Ras-Transfection into Mouse BW5147 T-Lymphoma Cells. *Cancer Research*. 47, 754-759.
- Colotta, Francesco, Paola Allavena, Antonio Sica, Cecilia Garlanda, and Alberto Mantovani. 2009. Cancer-related inflammation, the seventh hallmark of cancer: links to genetic instability. *Carcinogenesis*. 30(7), 1073-1081.
- DeCicco-Skinner, K.L., E.L. Trovato, J.K. Simmons, P.K. Lepage, and J. Wiest. 2010. Loss of Tumor Progression Locus 2 (TPL2) enhances tumorigenesis and inflammation in two-stage skin carcinogenesis. *Oncogene*. 30(4), 389-397.
- Dumitru, C.D., J.D. Ceci, C. Tsatsanis, D. Kontoyiannis, K. Stamatakis, J.H. Lin, C. Patriotis, N.A. Jenkins, N.G. Copeland, G. Kollias, and P.N. Tsichlis. 2000. TNF-alpha induction by LPS is regulated posttranscriptionally via a Tpl2/ERK-dependent pathway. *Cell*. 103(7), 1071-1083.
- Folgueras, Alicia R., Alberto M. Pendas, Luis M. Sanchez, and Carlos Lopez-Otin. 2004. Matrix metalloproteinases in cancer: from new functions to improved inhibition strategies. *The International Journal of Developmental Biology*. 48, 411-424.
- Furstenberger, G., D. L. Berry, B. Song, and F. Marks. 1981. Skin tumor promotion by phorbol esters is a two-stage process. *Proceedings of the National Academy of Sciences of the United States*. 78, 7722-7726.
- Gantke, Thorsten, Srividya Sriskantharajah, and Steven C. Ley. 2011. Regulation and function of TPL-2, and IκB kinase-regulated MAP kinase kinase kinase. *Cell Research*. 21, 131-145.

- George, A. and A. Salmeron. 2009. Cot/Tpl-2 Protein Kinase as a Target for the Treatment of Inflammatory Disease. *Current Topics in Medicinal Chemistry*. 9, 611-622.
- Gilmore, Thomas. 2011. NF- κ B Transcription Factors. Boston University Biology Department, Boston, Massachusetts. Last viewed March 2011. < <http://www.bu.edu/nf-kb/>>
- Hanahan, Douglas and Robert A. Weinberg. 2000. The Hallmarks of Cancer. *Cell*. 100, 57-70.
- Hatzia Apostolou, Maria, Georgios Koukos, Christos Polytarchou, Filippos Kottakis, Oksana Serebrennikova, Athan Kuliopulos and Philip N. Tsichlis. 2011. Tumor Progression Locus 2 Mediates Signal-Induced Increases in Cytoplasmic Calcium and Cell Migration. *Science Signaling*. 4, 55-66.
- Hayden, Matthew S., and Sankar Ghosh. 2008. Shared Principles in NF- κ B Signaling. *Cell*. 132, 344-362.
- Hu, Xueyou and Christine Beeton. 2010. Detection of Function Matrix Metalloproteinases by Zymography. *Journal of Visualized Experiments*. 45, 2445-2448.
- Inamdar, Gajanan, Subba Rao V. Madhunapantula, and Gavin P. Roberson. 2010. Targeting the MAPK pathway in melanoma: Why some approaches succeed and others fail. *Biochemical Pharmacology*. 80, 624-637.
- Lee, Jeung-Hoon, Kyung-Chae Kye, Eun-Young Seo, Kyungmoon Lee, Sang-Keun Lee, Jong-Soon Lim, Young-Joon Seo, Chang Deok Kim, and Jang-Kyu Park. 2008. Expression of Neutrophil Gelatinase-Associated Lipocalin in Calcium-Induced Keratinocyte Differentiation. *Journal of Korean Medical Science*. 23, 302-306.
- Lichti, U., J. Anders, and S. Yuspa. 2008. Isolation and short-term culture of primary keratinocytes, hair follicle populations and dermal cells from newborn mice and keratinocytes from adult mice for *in vitro* analysis and for grafting to immunodeficient mice. *Nature Protocols*. 3(5), 799-810.
- Lin, Cheng-Wei, Shing-Chuan Shen, Chih-Chiang Chien, Liang-Yo Yang, Lin-Ting Shia, and Yen-Chou Chen. 2009. 12-O-Tetradecanoylphorbol-13-Acetate-Induced Invasion/Migration of Glioblastoma Cells Through Activating PKC α /ERK/NF- κ B-dependent MMP-9 Expression. *Journal of Cell Physiology*. 225(2), 772-481.
- Karin, M., Y. Cao, F.R. Greten, and Z.W. Li. 2002. NF-kappaB in cancer: from innocent bystander to major culprit. *Nature Reviews Cancer*. 2(4), 301-310.
- Masson, Veronique, Laura Rodriguez de la Ballina, Carine Munaut, Ben Wielockx, Maud Jost, Catherine Maillard, Silvia Blacher, Khalid Bajou, Takeshi Itoh, Shige Itohara, Zena Werb, Claude Libert, Jean-Michel Foidart, and Agnes Noel. 2005. Contribution of host MMP-2 and MMP-9 to promote tumor vascularization and invasion of malignant keratinocytes. *The Journal of the Federation of American Societies for Experimental Biology*. 19, 234-236.

- McCawley, Lisa J., Jane Wright, Bonnie J. LaFleur, Howard C. Crawford, and Lynn M. Matrisian. 2008. Keratinocyte Expression of MMP3 Enhances Differentiation and Prevents Tumor Establishment. *The American Journal of Pathobiology*. 173, 1528-1539.
- Moore, R.J., D.M. Owens, G. Stamp, C. Arnott, F. Burke, N. East, H. Holdsworth, L. Turner, B. Rollins, M. Pasparakis, G. Kollias, F. Balkwill. 1999. Mice deficient in tumor necrosis factor-alpha are resistant to skin carcinogenesis. *Nature Medicine*. 5, 828-831.
- Morgan, David, David Welty, Adam Glick, David Greenhalgh, Henry Hennings, and Stuart H. Yuspa. 1992. Development of an *in Vitro* Model to Study Carcinogen-induced Neoplastic Progression of Initiated Mouse Epidermal Cells. *Cancer Research*. 52, 3145-3156.
- Nakashima, Shigeru. 2002. Protein Kinase Ca (PKCa): Regulation and Biological Function. *The Journal of Biochemistry*. 132, 669-675.
- Nelson, Thom, A.J. Riggs, Eric Endsley, and Vince Groppi. 2010. CellPlayer™ 96-Well Cell Migration Assay. Essen BioScience Biotechnology Group. Ann Arbor, Michigan. Last viewed March 2011.
<http://www.essenbioscience.com/documents/Essen_CellPlayer_CellMigration_AppNote_8000-0018-D.pdf>
- Nodwell, Trefor. 2003. Basal and Squamous Cell Carcinoma – A Review. Dalhousie University, Nova Scotia, Canada. Last viewed March 2011.
<www.medstudenttlc.com/2Fpresentation.php?Fid%3D56&ei=p9uJT56zNbKP0QHQ3MHRCQ&usg=AFQjCNEPtAJv0eWTW1qGWLpxNA4OctezQ&sig2=NR11g47ZMCep48OU3frLBQ>
- Pevsner, Jonathan. 2009. Bioinformatics and Functional Genomics. Baltimore, Maryland: Wiley-Blackwell.
- Pfaffl, Michael. 2001. A New Mathematical Model for Relative Quantification in Real-Time RT-PCR. *Nucleic Acids Research*. 29(9), 2002-2007.
- Ratushny, Vladimir, Michael D. Gober, Ryan Hick, Todd W. Ridky, and John T. Seykora. 2012. From keratinocyte to cancer: the pathogenesis and modeling of cutaneous squamous cell carcinoma. *The Journal of Clinical Investigation*. 122, 464-472.
- Shapiro, Steven D. 1998. Matrix Metalloproteinase degradation of extracellular matrix: biological consequences. *Cell Biology*. 10, 602-608.
- Snoek-van Beurden, Patricia A.M., and Johannes W. Von den Hoff. 2005. Zymographic techniques for the analysis of matrix metalloproteinases and their inhibitors. *BioTechniques*. 38(1), 73-83.
- Stulberg, Daniel L., Blain Crandell, and Robert S. Fawcett. 2004. Diagnosis and Treatment of Basal Cell and Squamous Cell Carcinomas. *American Family Physician*. 70(8), 1481-1488.

- Su, Fei, Amaya Viros, Carla Milagre, Kerstin Trunzer, Gideon Bollag, Olivia Spleiss, Jorge S. Reis-Filho, Xiangju Kong, Richard C. Koya, Keith T. Flaherty, Paul B. Chapman, Min Jung Kim, Robert Hayward, Matthew Martin, Hong Yang, Qiongqing Wang, Holly Hilton, Julie S. Hang, Johannes Noe, Maryou Lambros, Felipe Geyer, Nathalie Dhomen, Ion Niculescu-Duvaz, Alfonso Zambon, Dan Niculescu-Duvaz, Natasha Preece, Lúdia Robert, Nicholas J. Otte, Stephen Mok, Damien Kee, Yan Ma, Chao Zhang, Gaston Habets, Elizabeth A. Burton, Bernice Wong, Hoa Nguyen, Mark Kockx, Luc Andries, Brian Lestini, Keith B. Nolop, Richard J. Lee, Andrew K. Joe, James L. Troy, Rene Gonzalez, Thomas E. Hutson, Igor Puzanov, Bartosz Chmielowski, Caroline J. Springer, Grant A. McArthur, Jeffrey A. Sosman, Roger S. Lo, Antoni Ribas, and Richard Marais. 2012. RAS Mutations in Cutaneous Squamous-Cell Carcinomas in Patients Treated with BRAF Inhibitors. *The New England Journal of Medicine*. 366, 207-215.
- Werner, Sabine, and Richard Grose. 2003. Regulation of Wound Healing by Growth Factors and Cytokines. *Physiological Reviews*. 83, 835-870.
- Xue, Meilang, Patrick Thompson, Ian Kelso, and Chris Jackson. 2004. Activated protein C stimulates proliferation, migration, and wound closure, inhibits apoptosis and upregulates MMP-2 activity in cultures human keratinocytes. *Experimental Cell Research*. 299, 119-127.
- Yuspa, Stuart H. Anne E. Kilkenny, Peter M. Steinert, and Dennis R. Roop. 1989. Expression of Murine Epidermal Differentiation Markers is Tightly Regulated by Restricted Extracellular Calcium Concentrations *In Vitro*. *The Journal of Cell Biology*. 109, 1207-1217.